

**THE LATE PERMIAN STRATIGRAPHY OF THE UPPER
TWEEFONTEIN SECTION, EASTERN CAPE PROVINCE, SOUTH
AFRICA**

LANGWENYA, Mduzi, Department of Geology, Colby College, 5800 Mayflower Hill Drive, Waterville, ME 04901, mblangwe@colby.edu, **GASTALDO, Robert A.**, Department of Geology, Colby College, 5807 Mayflower Hill Drive, Waterville, ME 04901, **NEVELING, Johann**, Council for Geosciences, Private Bag x112, Pretoria, 0001, South Africa, **PREVEC, Rose**, Albany Museum, Rhodes University, Grahamstown, 6410, South Africa, **KAMO, Sandra L.**, Jack Satterly Geochronology Laboratory, Univ of Toronto, 22 Russell Street, Toronto, ON M5S 3B1, Canada, and **GEISSMAN, J.W.**, Department of Geosciences, University of Texas at Dallas, 800 West Campbell Road, Richardson, TX 75080

✓ CITATION IN BOTH TEXT AND
LITERATURE CITED
X CITATION NOT IN REFERENCES
OR VICE VERSA

I. ABSTRACT

The Karoo Basin of South Africa hosts a terrestrial record spanning the latest Permian and earliest Triassic. One critical boundary locality is Tweefontein in the Eastern Cape Province. This 100+ m section, ^{at} S 31° 49.334, W 24° 48.565, is reported as a transition from green Permian siltstones to mostly red Triassic siltstone. Our study complementing one lower in the section, focused on developing a high resolution stratigraphy of the upper 90+ m of a section near the original published coordinates (S 31° 49.089, E 24° 48.121). The project was to develop a high-resolution framework for complementary geochronologic and paleomagnetic stratigraphic studies, and provide a model for the depositional environments of paleontological assemblages.

Much of the section is covered but exposures are dominated by olive gray (5 Y 4/1), fining up, coarse to fine siltstone sequences. Carbonate cemented concretions occur in several horizons of olive siltstone from which a skull of *Dicynodon* sp. was collected. Siltstone color changes to grayish red (5 R 4/2) only near the top of the section. Here, TOC data from subjacent 15 m of olive siltstone, ranging from 0.3 - 6.6 %, indicate more algal than terrestrial biomass contribution. This TOC may reflect an abandoned channel fill complex that underwent pedogenesis and diagenetic overprinting, accounting for sediment reddening.

A zircon-bearing porcellanite occurs in a donga ~500 m to the west and is correlative at a stratigraphic height of ~65 m in our section. A suite of euhedral, sharply faceted grains was analyzed using CA-ID-TIMS with the ET535 EARTHTIME tracer. The $^{206}\text{Pb}/^{238}\text{U}$ weighted mean age of a coherent cluster of 5 concordant data for this lithology is 254.73 ± 0.24 Ma (late Wuchiapingian).

IS THERE SOME REASON WHY THESE ARE OMITTED FROM THE MANUSCRIPT, PROPER?

and TOC-TON RATIO VALUES

There are few localities in which long stratigraphic sections can be measured and our findings differ from those ^{previously} reported for the Tweefontein section. ~~Previous studies~~ ^{these} illustrate 40 m of Triassic red, concretionary mudstone interbedded with fluvial sandstone bearing intrabasinal pedogenic conglomerate lags in the upper part of the stratigraphy. In contrast, we record a predominance of olive gray siltstone and non-pedogenic conglomerate-bearing fluvial sandstone, constrained by geochronometric data to the latest Permian. ^{missed the point.}

II. INTRODUCTION

The Permian–Triassic (PT) mass extinction occurred about 252.17 ± 0.06 Ma (Shen et al., 2011), and it is generally accepted as the most extensive loss of life in Earth's history (Payne and Clapham, 2012). Researchers have suggested that this extinction event was more severe in the marine realm relative to terrestrial ecosystems. Recent estimates include a 90% loss of marine species (Black et al., 2012) and a 62.9% loss of terrestrial vertebrate families (Benton, 1995). After several decades of research focused on the PT extinction, opinions are still divided concerning other specifics of the event that may be central to its understanding.

Central to the controversy is the confusion over whether geochemical signatures at the Permian-Triassic Boundary (PTB) represent causes or effects of the extinction (Berner, 2002), along with the fact that the PTB is primarily defined by marine fossils and geochemical data in China (Retallack et al., 2005). Few researchers have attempted to correlate marine to terrestrial sediments (Twitchett et al., 2001). Recently, Rubidge et al. (2013) attempted a correlation of Late Permian vertebrate declines in the Karoo Basin, South Africa, and well-documented Lopingian marine vertebrate losses in South

China. They found no correlative vertebrate losses between the two sections. Without precise calibrations of Late Permian sediments in most non-marine sections, correlations of the PTB across non-marine strata remain controversial.

MIXED UP COERCIAL FLOW OF IDEAS

The Karoo Basin of South Africa consists some of the best-preserved sections to characterize and define the ^{Rocks below and above} terrestrial Permian-Triassic boundary. The Karoo basin is a retro-arc basin formed as result of subduction of the Pacific plate below southwestern Gondwana (Johnson, 2006). It is reported to have excellent exposures and a complete stratigraphic record of the continental PTB interval (De Kock & Kfischvink, 2004; Ward et al., 2000), although (Lindeque et al., 2007) reported discontinuities within and at contacts of some lithological layers. With a maximum thickness of 12 km, the basin spans the Late Carboniferous to the Early Jurassic (Johnson et al., 1996). The strata exposed in the Karoo Basin consist of the Dwyka Group, Ecca Group, Beaufort Group, Stormberg Group, and Drakensberg Group (Johnson et al., 1996). All strata, combined, are placed into the Karoo Supergroup.

Karoo Basin Stratigraphy

The Dwyka Group is the lowermost unit in the Karoo Supergroup; it spans the Late Carboniferous to the Early Permian (Johnson et al., 2006). It was formed from the accumulation of sediments that were likely deposited by melt-water from one or more major glacial icesheets on Gondwana during the migration of the supercontinent over the Carboniferous South Pole (Smith et al., 1993). It is composed of unsorted glacial debris, diamictites, and both sandstone and mudrock facies (Johnson et al., 2006). It is overlain by the Ecca Group.

• A FIGURE WOULD ASSIST THE READER IN FOLLOWING THE STRATIGRAPHY

The Ecca Group is comprised of sediments that accumulated in an extensive shallow sea during the Permian, subsequent to the melting of the Dywka glaciers (Johnson et al. 2006). It mainly consists of olive-grey mudstones and rhythmites with occasional intercalations of sandstones (Johnson, ~~1996~~). This sediment package indicates suspension load settling during the gradual infilling of the closed Karoo basin (Johnson et al., 2006). There is a transition to fully terrestrial deposits at the top of the Ecca Group.

The overlying Beaufort Group represents the transition from turbidite deposits to a continental setting (Smith, ~~1993~~). It is comprised of alternating mudstone-and-sandstone units with upward fining sequences, red-and-purple colors, abundant fossils, desiccation cracks and paleosol horizons. These are interpreted to indicate that floodplain aggradation dominated the sequence (Smith, ~~1993~~). The Beaufort Group is divided into two subgroups; the Adelaide Subgroup, which refers to the lower sedimentary units, and the Tarkastad Subgroup, which refers to the upper sediments. Rocks The two subgroups are further divided into five formations: the Adelaide Subgroup is comprised of the Koonap, Middleton, and Balfour formations, whereas the Tarkastad Subgroup is comprised of the Katberg and Burgersdorp formations (Johnson et al., 2006).

The Balfour Formation is the uppermost unit of the Adelaide Subgroup and it spans the PTB. It is dominated by sandstone and mudstone, which are characterized by sedimentary structures including planar and trough cross bedding and ripple cross laminations (Johnson et al., ~~2006~~). The Balfour Formation is comprised of five members. These are: the Oudeberg, Doggaboersnek, Barberskrans, Elandsberg, and

Palingkloof members (Catuneanu et al., 2005). The Palingkloof Member, which is the uppermost unit in the Balfour Formation, marks the first upward appearance of red mudstones (Johnson, 1976). Its contact with the underlying Elandsberg Member has been reported to mark the PTB (Retallack et al., 2003; Coney et al., 2007).

Permian-Triassic Boundary

The PTB is recognized by a lithological transition from primarily green siltstone to red siltstone, which is interpreted to reflect a facies transition in paleosols formed adjacent to meandering and then braided river systems (Smith, 1995). The facies change is interpreted as evidence for warming and drying, which lowered water tables, caused a massive vegetation die off, and subsequently led to low sinuosity rivers due to increased sedimentation and the absence of roots in the soils (Ward et al., 2000). The boundary is associated with the Last Appearance Datum (LAD) of the *Dicynodon* Assemblage Zone (Retallack et al., 2003), and a basin-wide event bed that was interpreted to separate Permian paleosols from Triassic paleosols at the lithological transition in the Balfour Formation (Ward et al., 2000). The boundary also is characterized by a negative excursion of carbon isotopes recorded from carbonate nodules and organic matter (Retallack et al., 2003), and an interval of reversed polarity (De Kock and Kirschvink, 2004). Recently, Gastaldo et al. (2009) disputed the traceability of the event bed across different localities throughout the basin.

Precise placement of the PTB at many localities across the central Karoo Basin is not yet established. The boundary is defined by a single detrital zircon date (252.5 ± 0.7 Ma, Coney et al., 2007), magnetostratigraphic sections at Commando Drift Dam (De Kock & Kirschvink, 2004) and Lootsberg Pass (Ward et al., 2005), and vertebrate-taxa

BUT WARD ET AL. USE THE SAME DATA TO PLACE THE PTB IN A NORMAL POLARITY INTERVAL

turnover to the *Lystrosaurus* Assemblage Zone proposed by Smith and Ward (2000). Other previous workers (Ward et al., 2000; Retallack et al., 2003) inferred the placement of the boundary from lithological models, which has resulted in problematic lithological correlations across the basin (Gastaldo et al., 2009). For example, Ward et al. (2000) placed the PTB along a nodular horizon below a laminated facies that is composed of dark-reddish brown and olive-gray mudstone couplets in what they termed the 'dead zone.' In contrast, Retallack et al. (2003) placed the PTB towards the top of the laminate event bed (see Retallack et al., 2003, their Fig.4) based on the presence of paleosols, nodules, and the LAD of the *Dicynodon* Assemblage Zone. Hence, no single lithostratigraphic feature appears sufficient to identify the boundary in the basin (Gastaldo et al., 2009, Ward et al., 2012 [technical comments]). Similarly, placing the boundary based on the *Dicynodon* LAD is not a standard scientific procedure because an index fossil for the continental PTB has not been formally established (Ward et al., 2005). Absolute dating of lithological units within the Palingkloof Member is needed to identify the boundary and allow for correlation with other sections.

This study presents a detailed stratigraphic investigation of a reported Permian-Triassic section (Ward et al., 2000) on the Blauwwater Farm 87 near Lootsberg Pass, Eastern Cape Province, South Africa. The results will detail sedimentary facies and paleosols, and discuss implications of a *Dicynodon lacerticeps* skull in the section. The study will also provide a zircon age for a porcellanite bed correlative with this locality.

III. LOCALITY

Fieldwork was conducted at the Blauwwater Farm 87, Eastern Cape Province, South Africa (Fig.1A). The farm is located on the west side of the N9 highway in between three

→??
DOESN'T SHOW
BOUNDARIES OF THE
EASTERN CAPE
PROVINCE

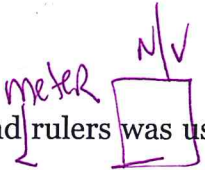
l.c.

WHAT ABOUT GASTALDO & NEVELING'S 2012 REPLY?

towns: Graaf-Reneit, Middleburg, and Nieu Bethesda (Fig.1B). The section begins at $S31^{\circ} 49.090 E24^{\circ} 49.120$ (Fig.1B), and is exposed mainly in dongas and erosional gullies that previously have been reported to expose the PTB (Ward et al., 2000). The locality was previously published as Tweefontein with GPS coordinates of $S31^{\circ} 49.334 E24^{\circ} 48.565$ (corrected for East latitude) (Ward et al., 2000). It was further correlated to PTB sections at Lootsberg, Old Lootsberg, Bethulie, and Caledon, using the LAD of the *Dicynodon* Assemblage Zone, the occurrences of isotopic anomalies, and the purported 'lamine' interval (Ward et al., 2005).

IV. MATERIALS AND METHODS

Field Work and Methods

A Jacob staff with a spirit level and  rulers was used to measure bed thickness to centimeter accuracy. It was initially placed at the top of the basal section reported by Spencer et al. (2013) and aligned at right angles to the bedding planes and a down dip of 2.5° . A clinometer on the Jacob staff was then opened to 2.5° , and an eyepiece was used to mark a point that is 1.5 m higher stratigraphically. For each 1.5 m, cm-scale rulers, 10x hand lenses, and Munsell color charts were used to characterize bed thickness, grain size, and lithologic colors, respectively. Primary structures, fining/coarsening sequences, and bed geometries associated with stratigraphic levels were recorded and described in field notebooks. Field descriptions were used to draw a rough stratigraphic column for reference purposes. The stratigraphic column was reworked at finer resolution at Colby College. In addition, photographs, hand samples, a zircon-bearing porcellanite, and a *Dicynodon* skull were gathered for laboratory analysis.

Laboratory Analysis And Methods

Thin sections: Hand samples, marked in the field indicating stratigraphic up, were sent to Applied Petrographic Services, Inc, where they were ground into standard thin sections for microscopic analysis. Polished thin sections were examined and photographed on a Leica DFC 290 microscope fitted with a Nikon camera and NIS Elements Version 3.00 imaging software. Point count sampling was used to count 300 grains per slide in transects, and determine grain size and sorting parameters in sandstone samples. Matrix and cement were not counted. An Olympus BX41 microscope was used to assess primary structures and diagenetic features, and to perform 300-point-counts in transects determine the proportion of quartz, feldspar, and lithics (QFL) for each thin section. The QFL proportions were plotted in a ternary diagram using Grapher 4 software.

Locality?
WHERE ARE THEY LOCATED?

UNKNOWN

Total Organic Carbon (TOC) and Total Organic Nitrogen (TON): A part of each siltstone sample was ground to powder, loaded into tin capsules, weighed, and burned in a 2400 Perkin Elmer CHN/O analyzer. Samples were run in a triplicate. To ensure data reliability, known acetanilide standards (C: 71.09% H: 6.71% N: 10.36%) were run as unknown among every 10 rock samples. Sample results were averaged and used to calculate ratios of TOC and TON (Table 4).

Stratigraphic Column: A stratigraphic column, detailing lithologies by grain size and Munsell colors, and illustrating primary structures, fining up sequences, bed contacts, a *Dicynodon* fossil, and a zircon-bearing porcellanite, was compiled from field descriptions using Corel X5 software. The stratigraphic column begins at the contact

→ DATA TABLES ARE NOT INTRODUCED IN THE M + M SECTION. ALSO TABLES ARE PRESENTED IN ALPHABETIC ORDER IN THE TEXT.

with thick channel sandstone at the top of the basal section reported by Spencer et al. (2013) and continues for 95 m up section.

Paleosols: A detailed paleosol classification scheme for Karoo paleosols is yet to be determined. There is a need to use a scheme applicable to all paleosols that will utilize features with greater odds of preservation, standardize paleosol names, and reduce subjective interpretations to yield paleosol names (Mack et al. 1993). To this purpose, Mack et al. (1993)'s paleosol classification scheme was used to identify and classify paleosols. It is based on six field noticeable pedogenic features that include organic matter content, horizonation, redox conditions, in situ-mineral alteration and illuviation of soluble minerals. (ite.)

Photographs: When possible, photographs from the field were merged into photomosaics using Adobe Photoshop CS6. With patchy exposures and limited lateral exposure at Blauwwater Farm, few photo mosaics could be constructed or traced to identify bounding surfaces and bed geometries.

Geochronology: Porcellanite samples were collected from a donga, which is located ~500 m to the west and correlative at a stratigraphic height of 65 m in our section. The samples were crushed and milled by standard rock processing methods, or in some cases, ash samples were milled in a blender or a ring mill. The procedure for concentrating heavy minerals on a Wilfley table was modified by re-processing the heavy concentrate until a significantly reduced sample size was achieved.

Pb and U isotopes in zircon were analyzed by CA-ID-TIMS (for 'chemical abrasion isotope dilution thermal ionization mass spectrometry') in the Jack Satterly Geochronology Laboratory at the University of Toronto. Zircon grains were pretreated

to remove radiation-damaged and altered zones ('CA'; Mattinson, 2005) by placing in a muffle furnace at $\sim 1000^{\circ}\text{C}$ for $\sim 24\text{-}48$ hours to anneal radiation damage, followed by partial dissolution in 50% HF in Teflon dissolution ($\pm 6\text{N}$ HCl) vessels at 200°C for approximately 6-17 hours, depending on the degree of visible alteration of the grains. Each zircon fragment was cleaned in HNO_3 , H_2O and acetone, and transferred to a miniaturized Teflon bomb (Krogh, 1973). Weights were estimated from grain measurements using photomicrographs. A mixed ^{205}Pb - $^{233}\text{-}^{235}\text{U}$ spike was added to the Teflon dissolution capsules during sample loading ('ET535' EARTHTIME community tracer, see www.earth-time.org, to facilitate inter-laboratory comparisons). Zircon was dissolved using ~ 0.10 ml concentrated HF acid and ~ 0.02 ml 7N HNO_3 at 200°C for 3-5 days, and re-dissolved in ~ 0.15 ml of 3N HCl. Uranium and lead were isolated from the zircon solutions using anion exchange columns, deposited onto out gassed rhenium filaments with silica gel (Gerstenberger and Haase, 1997), and analyzed with a VG354 mass spectrometer using a Daly detector in pulse counting mode or multiple Faraday collectors in static mode. Corrections to the $^{206}\text{Pb}/^{238}\text{U}$ and $^{207}\text{Pb}/^{206}\text{Pb}$ ages for initial ^{230}Th disequilibrium in the zircon data have been made assuming a Th/U ratio in the magma of 4.2.

All common Pb was assigned to procedural Pb blank. Dead time of the measuring system for Pb was 16 ns and 14 ns for U. The mass discrimination correction for the Daly detector is constant at 0.05% per atomic mass unit. Amplifier gains and Daly characteristics were monitored using the SRM 982 Pb standard. Thermal mass discrimination corrections are 0.10% per atomic mass unit for Pb and U fractionation is measured and corrected for each cycle. Decay constants are those of Jaffey et al. (1971).

THIS SEEMS TO HAVE BEEN BLOCK
COPIED FROM SANDRA'S REPORT WITHOUT
EDITING OR REWORDING

Age calculations were done using an in-house program by D.W. Davis. All age errors quoted in the text and table, and error ellipses in the Concordia diagrams are given at the 95% confidence interval. Plotting and age calculations were done using Isoplot 3.00 (Ludwig, 2003).

a. RESULTS

This section presents lithologies, lithofacies, the geochronology, biostratigraphy, and the lithostratigraphy of the upper interval at Blauwwater Farm 87. The section begins on top of a thick sandstone channel (Spencer et al., 2003) and continues upward with siltstones that are occasionally incised by lenticular sandstones.

Lithologies

Three lithologies (Table 1) widely occur throughout the section, namely fine and coarse siltstone, sandy coarse siltstone, and very fine sandstone.

Very fine sandstone: The majority of sandstone is of the very fine sandstone lithology. The lithology is interspersed as isolated beds at irregular intervals up the section. Most very fine sandstones have a quartz component of $\geq 50\%$ (Table 2, Fig. 2) with $>10\%$ matrix; these are classified as lithic sandstones. One sandstone sample (16.01.1, at 72 m) has a greater proportion of lithics (45%) than the proportion of quartz (39%), but it remains in the field of lithic sandstones (Fig. 2). Very fine sandstones have mean grain Phi sizes of 3.01-3.5 with standard deviations that range from 0.31 to 0.53 (Table 2). Fining upward sequences characterize most sandstone bodies (Fig. 12). Grain size statistics indicate very fine grain sizes and moderate to well sorting. The very fine sandstones are yellowish brown (10YR 8/3), greenish gray (5GY 7/1) and light olive gray (5Y 5/1) in color. The sandstones have bedding that ranges from 15 to 80 cm in

MIGHT NOT THE FINE SILTSTONE ACTUALLY BE A DIFFERENT Lithology than the coarse siltstone? ARE THERE ANY BEDS THAT INTEGRATE THE TWO GRAIN SIZES?

Repetition

ORDERING IS NOT LOGICALLY PRESENTED

SAND: SILTSTRATIO (TABLE 2)

WHICH ARE WHAT?

AND THIS ϕ SIZE CLASSIFIES IT AS WHAT?

WACKES!!

These are

Fig. 12 can not be presented after Fig. 7. It must be Fig. 3!

Implies that other SS lithologies exist but are not treated in the paper.

THE REASON WEAR LEARN THAT THESE ARE LITHIC WACKES -

thickness. There are also laminated and cross-bedded sandstones (Fig.3A) showing lenticular and tabular bed geometries. Beds may exhibit soft-sediment deformation structures (Fig.11) and isolated scattered mud clasts.

Sandy coarse siltstone: The sandy coarse siltstone lithology primarily overlies thick sandstone channel at the top of the basal section reported by Spencer et al. (2013), and its occurrences are limited at higher stratigraphic positions. Sand-sized grains floating in masses of silt-sized grains, matrix and cement define this lithology. The sand-sized grains are mainly sub-angular quartz. Sandy coarse siltstone is olive gray (5Y 4/1) or greenish gray (5GY 4/1) in color. It may contain plane bed laminations, trough and planar cross bedding, ripples (Fig.3C), and millimeter-scale mud clasts (Fig.4C). Bed thicknesses range 3 cm to 30 cm. Isolated bioturbation (Fig.3B) is found under thin sections.

Fine and coarse siltstone: The fine and coarse siltstone forms a comparative major part of the upper interval at Blauwwater Farm 87. This lithology occurs in discontinuous zones throughout the section. It is colored in shades of olive green (5Y 4/1), brownish grey (5YR 4/1) and greenish grey (5GY 6/1). Occasionally, the fine and coarse-grained lithology is mottled (Fig.4B). It may comprise of laminated beds, massive (homogenous) deposits, fining upward sequences, and lenticular bed geometries. Cm-scale calcite cemented nodules (Fig.4A, 4B) are commonly found in this lithology in the outcrop. Bioturbation is generally present under thin sections.

Lithofacies

Four lithofacies associations are identified based on a compilation of field-and-laboratory descriptions of grain sizes, geometries, and sedimentary and biogenic structures to delineate different bed forms. The sedimentology is dominated by very

fine-grained sandstone, sandy siltstone, lenticular siltstone, and homogenous siltstone facies (Table 3, Fig. 12).

CAN NOT FOLLOW FIGURE 4 -

Very fine-grained sandstone Facies: This facies consists of lenticular, cross-bedded units of very fine sandstone (Fig. 3A, 4D). It occurs in beds of yellowish brown (10YR 8/3), greenish-gray (5GY 7/1), or light olive-gray (5Y 5/1). Beds are normally up to 40 cm thick, but may thin laterally. Sandstones have an overall fining upward trend, forming both single and multi-storey units. Beds display a variety of primary structures including rippled tops, soft sediment deformation structures (Fig. 11), and mm-and-cm scale trough cross beds (Fig. 3A, 10). Paleocurrent plots of trough cross-bed axes measurements yield a northwest flow (307°) direction (Fig. 5). Secondary features include abundant organics, and millimeter-scale mud clasts. Lower contacts are erosional towards the underlying siltstone, and reveal slightly inclined bounding surfaces upon tracing. Upper contacts are generally sharp. One very fine sandstone unit at 72 m exhibits a tabular sandstone bar form.

Interpretations: The lenticular bed geometries indicate deposition in river channels that flowed to the northwest (Fig. 5). The very fine sandstone facies is therefore interpreted as deposits of several rivers that were bordered by floodplains, which during overbank flooding received unchanneled sand and silt, and resulted in the overlying sandy coarse siltstone facies. The presence of soft-sediment deformation structures AT 84 m indicates water-saturated conditions during deposition. The overall fining upward trend is indicative of waning flow energy over time. However, the tabular form of the cross- and ripple-bedded sandstone bed at 72 m indicates an isolated episode of high-energy deposition. Slightly inclined bounding surfaces indicate pauses in deposition, which is substantiated by mud-draped contacts and rippled tops. The mud clasts are

How are these determined?

THIS SEEMS OUT OF PLACE LOGICALLY

MIS NUMBERED

* HOW AND THE STRATIGRAPHIC HEIGHTS OF THESE BE IDENTIFIED FOR THE READER?

WHERE? 84 M OR ELSEWHERE?

indicative of seasonal precipitation and the presence of flash or seasonal floods (Rust & Nanson, 1989).

Sandy Siltstone Facies: This facies comprises of sandy coarse siltstones that are either dark greenish gray (5GujoY 4/1) or light olive gray (5Y 5/2) in color. It usually overlies fluvial channel sequences and is overlain by finer siltstone sediments (Fig. 12).

BUT THIS IS NOT A DEFINED LITHOLOGY. COARSE-MID FINE SILTSTONE IS THE ONLY DEFINED OPTION

This facies tends to fine upward with upper contacts being gradational with overlying fine siltstone facies. Lower contacts are generally erosional and sharp with underlying

sandstone. Beds display ^{??} bands of sand and silt, but a 300-grain count analysis of a sampled bed at 68 m (thin section 19.01.6) indicates a higher proportion of silt than

sand. Beds have maximum thicknesses of 80 cm, and exhibit sandstone lenses and siltstone lamina. Primary structures typically include thin (1-5 mm) horizontal, or

slightly inclined (<3°) laminae. A tracing of bounding surfaces reveals an isolated presence of climbing dunes at 33 m (Fig. 6). Secondary features include lenticular bed

geometries, organic matter, and mm-scale sub-angular mud pebbles (Fig. 4C). The latter feature is abundant towards contacts.

IF THIS IS TRUE, WHY IS IT PLACED HERE TO DEMONSTRATE THE SANDY SILTSTONE FACIES?

Results of TOC and TON analyses on sandy coarse samples from 38 m, 42 m, and 68 m stratigraphic levels indicate that carbon content ranges from 0.32 to 0.75, and

nitrogen content that ranges from 0.017 to 0.068 (Table 4). Most TOC: TON ratios fall below 10, with the exception of 45.11 at 68 m. The results show algal origins of organic

matter at 38 m and 42 m, and terrestrial origins of organic matter at 68 m (Brown et al., 1998).

Interpretations: This facies assemblage is considered to represent channel fill deposits. The sharp erosive bases suggest sudden deposition of sediments during floods, followed by a gradual decrease in current energy, which resulted in the characteristic

occurrence

? WHAT DOES THIS MEAN? REALLY?

value of

INDICATE

OK. IN PROPER ORDER

grading, laminations, and climbing dunes observed ~~in this facies~~. The angular mud clasts and organics may be related to the scouring and erosion of the preexisting material during the floods.

WHERE IN THE LANDSCAPE?

Lenticular Siltstone Facies: This facies consists of alternating sequences of

lenticular fine and coarse siltstone exhibiting primary structures. Fine siltstones are olive gray (5Y 4/1), dark greenish gray (5GY 4/1), or brownish gray (5YR 4/1). They display primary structures that include abundant millimeter-scale parallel laminations, planar cross-beds, and asymmetrical ripples. Beds display lenticular bed geometries and generally have a 'rubbly' appearance in the field. This facies can be distinguished from the homogenous siltstone facies by the absence of nodules and/or color mottling. Coarse siltstones are typically dark greenish gray (5GY 4/1), light olive gray (5Y 7/2), or brownish gray (5YR 4/1). Beds are cm-scale in thickness, and well cemented. Primary structures include planar cross beds in cm-scale set, horizontal lamination and minor ripple laminations. Most beds display lenticular geometries exhibiting erosional lower contacts. Like fine siltstones, coarse siltstones lack pedogenic features such as nodular

BIT CONFUSING. ARE THESE INTERNAL TO THE LENTICULAR BED GEOMETRY?

horizons and color mottling.

THIS SEEMS OUT OF PLACE LOGICALLY

WHAT ARE THE GEOMETRIES OF OTHER BEDS?

CHN analysis of a lenticular siltstone sample gives 0.37 in carbon, and 0.092 in nitrogen (Table 4: sample 19.01.9). These carbon and nitrogen values give a TOC: TON ratio of 4.11. TOC/TON ratios <10 indicate an origin of organic matter from marine algae (Brown et al., 1998). With a TOC: TON ratio of 4.11, the lenticular siltstone facies has an aquatic source.

RESULTS IN VALUES OF
AA RESULT

?? DO YOU MEAN THE ORGANIC MATTER THEREIN?

Interpretations: This facies represents overbank floodplain deposits. These lens-shaped deposits represent discontinuous ripple or dune crests and troughs, resulting from sediment deposition in a low energy setting, punctuated by high-energy sediment

CHANNEL-FILL COMPLEX?

THEN, HOW DO YOU EXPLAIN THE ABSENCE OF PEDOGENIC FEATURES? WHY HAVEN'T THESE SEDIMENTS UNDERGONE SOIL FORMATION?

OR INSUFFICIENT COARSER BEDDING SEDIMENT.

deposition from sporadic storm floods. These discontinuous ripples or dunes formed during period of high-energy current, which had inadequate time to form complete ripples, resulting in this facies.

Homogeneous Siltstone Facies: This facies consists of fine and coarse siltstone that has undergone pedogenic alteration. It occurs in light olive gray (5Y 4/1), dark greenish gray (5GY 4/1), greenish grey (5GY 6/1), or brownish gray (5YR 4/1).

Massive and homogenous bedforms, along with extensive bioturbation in thin sections (Fig. 3B) define this facies. Burrowing organisms or roots have destroyed original stratification. There are rare cross-laminated lenses and streaks of sandstone, but thin bedding is generally absent. The facies occurs as heavily weathered beds up to 30 cm

How can you tell one process from another

in thickness. Mud-draped bedding planes and organic matter are generally recognizable in the field and in thin sections. Homogenous siltstones also exhibit mottled patches of brownish gray and greenish siltstones (Fig. 4B), and interspersed iron and magnesium, or carbonate-cemented, mm-cm scale nodules. The nodules are concentrated in discrete horizons (Fig. 12).

AGAIN - FIGURE IS OUT OF CONSECUTIVE ORDER

CHN analysis of homogenous siltstone samples gives 0.11 to 0.93 in carbon, and 0.02 to 0.34 in nitrogen (Table 4: samples 1-50, 19.01.3, 19.01.4 and 19.01.8). TOC: TON ratios all fall below 10, with the exception of ratios 17.33 and 17.5, at 47 m and 126.8 m, respectively. TOC: TON ratios <10 represent organic matter from marine algae, whereas TOC: TON ratio of $10 > x > 10$ suggest an occasional terrestrial plant source of organic matter (Brown et al., 1998).

Interpretations: Siltstone containing nodules, exhibiting homogenous and massive bed forms, and color mottling were interpreted as paleosols. Three paleosol types were identified using the criteria of Mack et al. (1993)'s paleosol classification

→ THESE. MAINTAIN A CONSISTENT TENSE IN THESE SECTIONS.

scheme. First, homogenous siltstone scattered with non-calcareous nodules of iron and manganese oxide and color mottling were interpreted as hydromorphic gleysols. Second, siltstone exhibiting both calcareous ^{-cemented} nodules and color mottling – irregular patches of olive gray (5Y 4/1) mixed with brownish gray (5YR 4/1) – were interpreted as Gleyed Calcisols. Third, homogenous siltstone with scattered brown cylindrical and carbonate-cemented nodules were interpreted as Stage II Calcisols.

WHAT'S THE DIFFERENCE HERE?
BOTH HAVE A CARBONATE COMPONENT

Unknewed presentation

Paleosols at the Earth's surface are in direct contact with the atmosphere, and thus can be used to interpret paleoclimates (Sheldon and Tabor, 2009). The presence of hydromorphic gleysols is interpreted to represent a humid, nearly ever-wet climate, based on color mottling (Mack et al., 1993). Color mottling occurs in areas with high water tables that fluctuate over short periods of time. Fluctuations cause alternating oxidizing and reducing conditions, resulting in irregular patches of brown and green colors (Mack et al., 1993).

TENSE?

good

The presence of Gleyed Calcisols suggests that a composite paleosol formed under fluctuating hydrologic conditions. The duration of fluctuations may have been seasonal or multi-year. The Gleyed Calcisols is composite in that a soil layer was buried by subsequent increments of sediment (Wright and Marriot, 1996). Gleying and calcification are consistent with soil development under conditions of a greatly variable distribution of precipitation. Waterlogged soils would characterize humid intervals, whereas a periodic drawdown of water tables during arid climates would allow color mottling and nodules to form.

grammar

The literature provides divergent paleoclimatic interpretations of calcisols in the central Karoo Basin. For example, Ward et al. (2005) interpreted paleosols bearing nodules as indicative of arid conditions, whereas Retallack et al. (2003) interpreted

HOW ABOUT SEASONABLY DRY?? WHY ARID??
CHECK DEFINITIONS BASED ON THE AMOUNT OF RAIN FALL PER YEAR -

THIS IS DISCUSSION MATERIAL PRESENTED IN THE RESULT SECTION

WHERE IS THE DESCRIPTION OF STAGE II CALCISOLS?
THIS IS MISSING -
Referred to on pg. 24

carbonate nodule-bearing paleosols, such as Bada, Hom and Som types, as indicative of stagnant groundwater conditions. Therefore, carbon and oxygen isotopic data from the nodules are needed to determine if the Calcisols in this section indicate wet or dry conditions (Tabor et al., 2007).

Geochronology

Abundant zircon was recovered from the porcellanite sample collected from a donga (Fig. 7A) that is ~500 m to the west and correlative at a stratigraphic height of 65 m in our section. The GPS location of the porcellanite bed is S31° 49.090, E24° 49.116. Zircons include euhedral elongate crystals, equant multi-faceted grains, and many mechanically-rounded, frosted, detrital grains (Fig. 7B). Detritally-rounded rutile is also present in trace amounts, as is titanite. Particular attention was paid to selecting sharply-faceted grains that show little surface abrasion from transport and that may have been deposited during a volcanic eruption. These grains gave concordant data with a suite of $^{206}\text{Pb}/^{238}\text{U}$ ages ranging from 277.8 ± 0.9 Ma to 256.98 ± 0.27 Ma based on the average of two grains with ages of 257.0 ± 0.3 Ma and 256.8 ± 0.5 Ma (Fig. 8A). A younger coherent cluster of 5 concordant data gives a weighted mean age of 254.73 ± 0.24 Ma (Fig. 8A, 8B). This is interpreted as a maximum age for the time of deposition of the unit.

Biostratigraphy

A *Dicynodon lacerticeps* skull was excavated from a carbon cemented concretionary olive siltstone interval about 300m to the west and correlative at the 81 m stratigraphic level (Fig. 7C, 7D). The GPS location of the skull is S31° 49.055, E24° 49.528. The *Dicynodon* Assemblage Fauna has been used to define the latest Permian

THIS SEEMS TO HAVE BEEN BLOCK
COPIED FROM SOMEONE'S
REPORT

WHO IDENTIFIED
THIS SPECIMEN?

of the SECTION UNDER STUDY

ZONE

vertebrate biozone (Rubidge et al., 2013), and marks the upper position of the Permian-Triassic boundary in the Karoo Basin (Smith and Ward, 2001).

Stratigraphy

The upper Blauwwater interval is predominantly comprised of fine and coarse siltstone with fining upward sequences that range from fine sandstone to fine siltstone (Fig. 12). Rippled and cross-bedded lenticular sandstone occasionally pinches out within the siltstones. Both sandstone and siltstone lithologies are yellowish brown (10YR 8/3), greenish gray (5GY 6/1), brownish gray (5YR 4/1), or olive gray (5Y 4/1) in color. Siltstone colors change from greenish-gray (5GY 4/1) or olive-gray (5Y 4/1) to predominantly brownish gray (5YR 4/1) at the 121 m stratigraphic level, near the top of the section. Occasional color mottling, calcite-cemented nodule horizons, mud-clasts, organic matter, bioturbation, and planar and lenticular bed geometries characterize the lithologies. Fossils include a single *Dicynodon lacerticeps* skull that was collected ~500 m west of our section at a correlative 81 m stratigraphic level (Fig. 7C, 7D). The presence of the skull suggests that the Blauwwater section is Late Permian, according to published biostratigraphic models (Rubidge et al., 2013).

V. DISCUSSION

Stratigraphy: A ~95 m interval near published GPS coordinates (S31° 49.334 E24° 48.565 by Ward et al., 2000) was sectioned. This interval has been reported to consist of basal olive mudstone and upper concretionary red mudstone, which are both interbedded with sandstone (Ward et al., 2000, their Fig. 1). The PTB was placed at a color transition from olive to dominantly maroon inter-channel silt and mudstone facies. A change from seasonally wet to seasonally arid conditions is interpreted across the PTB on the basis of a change in sandstone and shale architecture from meandering

THIS IS REALLY A REPEAT OF WHAT CAME PREVIOUSLY. THERE ARE NO TRENDS IDENTIFIED BASED ON THE CYCLICITY OF DEPOSITIONAL ENVIRONMENTS. THERE IS NO MENTION OF THE LOCATION HIGH DENSITY SAMPLING EXCEPT IN THE ABSTRACT. WHERE ARE THESE DATA? WHERE DO THEY FIT INTO THE GRAND SCHEME OF THINGS?

REQUIRES SOME INTRODUCTORY TEXT TO BEGIN A DISCUSSION

REALLY - MUDROCK ARCHITECTURE?

to braided rivers (Ward et al., 2000, Smith and Ward, 2001). The PTB also is reportedly located at the base of a laminate interval, which consists of dark reddish-brown and olive-gray mudstone couplets (Ward et al., 2000). This laminate event bed is reportedly traceable across Lootsberg, Old Lootsberg, Bethulie and Caledon sections based on the LAD of *Dicynodon* (Ward et al., 2000), and carbon isotopic data reported from Bethulie and Caledon (Ward et al., 2005). However, Gastaldo et al. (2009) demonstrated that the laminate interval is neither unique nor traceable across the different localities in the central Karoo Basin. This discrepancy in the lithological model necessitates high-resolution descriptions of critical PTB stratigraphic sections such as Blauwwater Farm 87.

The lithostratigraphy observed at Blauwwater Farm 87 in the current study contradicts descriptions reported by Ward et al. (2000). ~~Ward et al. (2000)~~^{THEY} reported a total of ~100 m section with ~50 m maroon concretionary mudstone, ~ 20 m olive mudstone, and ~ 30 sandstone. In the current study, most of the ~95 m section (Fig. 12) is covered, but the majority of exposed dongas occur in color shades of olive-gray (5Y 4/1) and greenish-gray (5GY 4/1). These colors change to predominantly brownish-gray (5YR 4/1) within the last ~6 m of the ~95 m section. No concretions were observed within this continuous brownish-gray siltstone interval as reported by Ward et al. (2000, their Fig. 1).

Ward et al. (2000) identified the PTB based on the stratigraphic presence of a laminite event bed within a sandstone-shale interval. The laminite bed is described as void of evidence of life (Smith and Ward, 2001) and integral to Permian-Triassic mass extinction models (Gastaldo et al., 2009). We found no laminite event bed at the

lithological color transition from greenish to brownish gray siltstone. This discrepancy raises questions about the laminite bed stratigraphic marker of the PTB, and necessitates refinement of the published lithostratigraphical models of the PTB across several central Karoo localities.

Paleosols: Paleosols provide evidence for phases of sub-aerial exposure and modification of sediments and, thus, are powerful tools for a variety of paleoenvironmental purposes (Wright, 1992). Despite such importance, few researchers have reported on paleosols in the central Karoo Basin (Smith 1995; Retallack et al., 2003).

Smith (1995) characterized paleosols of a Permian-Triassic transition sequence ^{IN} the Bethulie District. ^{WHERE} Two *Dicynodon* Assemblage Zone paleosols are reported. These are ^{AN} hydromorphic gleysol and immature entisol. Hydromorphic gleysol are described as the most common paleosol, and characterized by color mottling, root traces, gypsum rosettes, septarian nodules, and disarticulated skeletal remains of ^{THE} *Dicynodon* Assemblage fauna. These gleysols are interpreted to have formed on floodplain lake and pond deposits (Smith, 1995). Immature entisols are comprised of maroon clay-rich horizons, slickensides, vertical root traces, smooth topped calcareous nodules, and rhizoconcretions. This paleosol is interpreted to have formed on proximal floodplains (Smith, 1995). In contrast, one *Lystrosaurus* Assemblage Zone calcitic paleosol was identified ^(SMITH, 1995) on the basis of desiccation cracks; green mottles around rhizoconcretions; and a greater abundance of calcareous nodules relative to those found in the *Dicynodon* AZ paleosols. Desiccation cracks and nodule morphologies, which are similar to those of modern calcretes, are interpreted to indicate an increasingly semi-arid climate with highly seasonal precipitation.

BUT, AREN'T THESE CHARACTERISTICS OF UERTISOLS? SEE MACK ET AL. (1993) AND OTHERS

DOESN'T FIT THE TYPICAL SENTENCE

MISUSE OF A SEMI-COLON

Retallack et al. (2003) offered a more detailed description of Late Permian and Triassic (paleosols in the Karoo basin based on limited criteria of lithological characteristics and color. They identified 6 protosols (Zam, Pawa, Hom, Du, Patha, and Barathi) 4 calcisols (Bada, Som, Kuta, and Karie), and 2 gleysols (Sedibo and Budi) that span the Permian-PTB at Bethulie, Carleton Heights, and Lootsberg Pass. Permian paleosols include Bada, Du, Hom, Pawa, Som, and Zam, and are described as purple and bluish in color.

Bada paleosols are described as gray siltstone with shallow and scattered calcareous nodules and rhizoconcretions (Retallack et al., 2003, their Table 1). They are reported to have formed under semi-arid and long, dry conditions. In contrast, Bada paleosols are also described as gleyed soils consisting of blue-gray silt comprising of large calcareous nodules (Retallack et al., 2003, p1141 in text). They are also interpreted to represent ^{Pedogenesis in} floodplain depressions with semi-arid and long, dry seasons. The two descriptions of the same paleosol are contradictory.

Hom Paleosols are described as white sandstone with shallow and scattered calcareous nodules and rhizoconcretions (Retallack et al., 2003, their Table 1). This description is indistinct from that of Bada paleosols, except for more abundant relict bedding in Hom paleosols. Both paleosol types are reported to have deep root traces, calcareous nodules, and interpreted to have formed under low water table conditions (Retallack et al., 2003, pg.1143 in text). The absence of distinctive features ~~distinctive features~~ and inconsistencies make it hard to independently recognize Hom paleosols elsewhere. Proof
READ
THE
TEXT

Zam paleosols are described as bedded purple-gray siltstone with fine roots traces and burrows (Retallack et al., 2003, their Table 1). They are reported to have had

vegetation dominated by quillworts, which thrive under water or wet meadows (Retallack et al., 2003, pg1146). However, Zam paleosol paleoclimatic conditions also are reported as unknown (Retallack et al., 2003, their Table 1), which raises questions about the basis of designating a lake margins paleotopography for ~~Zam~~^{them} paleosols (Retallack et al., 2003, their Table 1).

Som paleosols are described as gray siltstone surfaces over purple siltstone with shallow calcareous nodules (Retallack et al., 2003, their Table 1). However, Bada paleosols are also described as blue-gray/dark-greenish sandstone (GSA repository # 2003122), and comparable to Hom, a white sandstone (Retallack et al., 2003, pg. 1141 in text). Such discrepant paleosol descriptions make it hard to recognize the paleosols elsewhere.

Three Late Permian paleosols are identified in the current study using the classifications of Mack et al. (1993). These are gleysols, gleyed calcisols and stage II calcisols. Gleysols are defined as horizons with low Chroma colors, such as gray and green, nodules of iron and manganese oxide, and color mottling (Mack et al., 1993). Siltstone at 42 m, 116 m, and 120 m stratigraphic levels at Blauwwater exhibit mottled patches of brownish-gray (5YR 4/1) and olive-gray (5Y 4/1). Non-calcareous, weathered nodules of iron and manganese oxide are also observed at the 120 m stratigraphic height. These irregular siltstone intervals are identified as gleysols and resemble Smith's (1995)'s hydromorphic gleysols at Bethulie District. Hydromorphic gleysols are the most common paleosols within the Dicynodon AZ at Bethulie, and are described as having pervasive color mottling, root channels, septarian nodules, and gypsum rosettes (Smith, 1995). In contrast to Bethulie hydromorphic gleysols, no root channels or gypsum rosettes were observed in gleysols at Blauwwater.

See pg. 18!!

ital.

WHAT ARE THE CONDITIONS NECESSARY FOR GYPSUM TO BE PRECIPITATED. IS THEIR PRESENCE CONSISTENT WITH WET SOIL CONDITIONS?

THIS IS PRESUMED BECAUSE YOU DID NOT COLLECT A SAMPLE NOR DID YOU CONDUCT XRD ANALYSES TO DETERMINE THE MINERALOGICAL AND CHEMICAL COMPOSITION OF THE FEATURES.

Gleyed calcisols are paleosols in which a calcic horizon is prominent but also display evidence of periodic waterlogging, such as mottles of drab colors, ~~according to~~ Mack et al. (1993). An isolated siltstone interval at 91-92 m stratigraphic level, which exhibits both carbonate-cemented nodules and drab color mottling, is characterized as a gleyed calcisol. None of Retallack et al.'s (2003) Late Permian paleosols at Bethulie, Calton, Heights and Lootsberg Pass, or Smith (1995)'s *Dicynodon* AZ paleosols are similar to the gleyed calcisols. The differences can be attributed mainly to different paleosol classification schemes that are solely based on color and lithology, and often include primary structures (Smith, 1995; Retallack et al., 2003).

Calcisols are paleosols with subsurface horizons enriched in carbonate (Mack et al., 1993). Siltstone at 42 m, 52 m, and 97 m stratigraphic levels have scattered brown, carbonate-cemented nodules (40 cm max diameter), and are characterized as calcisols. Siltstone intervals with scattered carbonate nodules correspond to stage II calcisols (Mack et al., 1993). Neither Retallack et al. (2003) nor Smith (1995)'s Late Permian paleosols are similar to the Blauwwater calcisols. Only Sedibo, a Triassic gleysol described by Retallack et al. (2003) as a greenish-gray siltstone exhibiting deep, well-focused calcareous nodules, resembles Blauwwater calcisols paleosols. However, no information is provided about Sedibo nodules, which would allow for comparison with nodules at Blauwwater.

Depositional Environment Interpretations: ^{THE} Sedimentary facies determined at Blauwwater suggest an aggradational floodplain, adjacent to fluvial channels of the Late Permian. Occasional flood events inundated the floodplain, raised water tables, and deposited silt in abandoned channels and overbanks. ^{Settings} Sedimentary facies include very

SHOULD I SOME OF THESE RESULTS HAVE BEEN PRESENTED ON PAGE 18?

fine-grained sandstone facies, sandy siltstone facies, lenticular siltstone facies, and homogenous siltstone facies.

Very fine-grained sandstone facies consists of lenticular, rippled, and cross-bedded units of very fine sandstone, which are interpreted to be fluvial channel deposits based on sedimentary structures. Sandstone bodies with erosional bases and sharp tops (upper contacts) form channel like deposits. Primary structures such as current-rippled cross-laminated sandstone are considered to have formed by traction and suspension deposition. Similar facies of lenticular, rippled and cross-bedded sandstone at Wapadsberg, Lootsberg, Tweefontein, Old Lootsberg, and Bethulie are interpreted to represent highly sinuous fluvial systems during the late Permian (Smith, 1995; Ward et al., 2000). Overlying this facies association is the sandy siltstone facies.

The sandy coarse siltstone facies is characterized by bands of sandstone lenses and siltstone lamina, and is interpreted to represent channel-fill deposits based on sedimentary structures and facies distribution. It mainly overlies sandstone lithofacies. Siltstone lamina within beds of sand and silt suggest periods of low energy conditions, and deposition from suspension during channel abandonment. Sandstone lenses within the facies association were introduced during periodic flood events. Fining upward sequences suggests variation of current energy.

The lenticular siltstone facies is characterized by alternating fine and coarse siltstone sequences that exhibit primary structures but no pedogenic features. This facies association is interpreted to represent floodplain overbank deposits based on sedimentary structures and facies distribution. It maybe attributed to deposition from extensive overflow of fluvial systems of the Late Permian. Parallel and cross-laminated siltstones were probably deposited on top of often-underlying sandy siltstone beds

→ ASGAW, How does it happen that overbank, floodplain deposits do NOT GET subjected to pedogenesis? EVER?

ALL of THIS IS UNREFERENCED

MUCH of THIS IS A REPEAT of THE INTERPRETATION SECTION PREVIOUSLY PRESENTED. HOW ABOUT SOME COMPARATIVE AND SYNTHETIC TEXT-

Doesn't this make them also CHANNEL fill deposits?

associated with abandoned channel and floodplain conditions, during period of low current energy.

Previous sedimentology studies of PTB localities in South Africa have highlighted a facies changeover from high sinuosity to low arid sinuosity fluvial river systems, along the lithological color transition to dominantly maroon siltstone (Smith, 1995). Ward et al. (2000, their Fig.1) extended the observation by demonstrating that the facies change is basin-wide. No facies change is observed at the onset of reddening siltstone at Blauwwater. This is expected given that Blauwwater is a Wuchiapingian section, not a PTB section as suggested by Ward et al. (2000). However, the suggestion that the facies change to braided stream architecture is traceable basin-wide at the lithological color transition is questionable.

NOT LOGICALLY PRESENTED

Paleoenvironmental Interpretations: Previous researchers have interpreted the presence of shallow nodules and channel architecture in Late Permian strata as indicative of arid and seasonally fluctuating climatic conditions (Ward et al., 2000; Retallack et al., 2003). A lithological association of maroon siltstone in the central Karoo strata has been interpreted to indicate cooler temperatures and wetter conditions (Tabor et al., 2007) or warmer temperatures (Retallack et al., 2003). However, the inconsistent paleosol descriptions by Retallack et al. (2003) identified in this study may suggest that their warmer climate hypothesis is questionable.

AND WETTER CONDITIONS

INTERPRETATION?

Interspersed gleysols, gleyed calcisols, and calcisols at irregular intervals throughout the upper Blauwwater interval potentially record high-frequency paleoclimate fluctuations, and may be indicative of strong seasonality in the Late Permian, an interpretation similar to others.

"Tweefontein"

REFERENCES!!

ACTUALLY, THIS PAPER INTERPRETS AN INCREASING WET TRENDS RATHER THAN ARIDIFICATION.

NOT REALLY DISCUSSED OR DEMONSTRATED TO BE IRREGULAR

Blauwwater paleosols formed under at least two fundamentally different paleoclimatic conditions characterized by gleysols and calcisols. Gleysols are characterized by low Chroma colors and extensive mottled horizons. These mottles are typical of humid, nearly ever wet regions, and probably indicate processes related to periodic rise and fall of water tables, or seasonal flooding from overland flooding (Mack et al., 1993). Stage II calcisols at Blauwwater are characterized by scattered calcite-cemented nodules. A pedogenic origin for these nodules has not been established; nevertheless, they form *in situ*, in a carbonatic, poorly drained system in a semi-arid environment (Sanz et al., 1996). The calcisols may reflect conditions of aridity that existed at least seasonally during the Late Permian.

TOC: TON values (Table 4) calculated from Blauwwater samples are mostly under 10, with a few values greater than 10, representing mostly algal and occasionally terrestrial plant signatures of organic matter. Paleosols with algal signatures likely formed in high water table conditions while those with terrestrial plant signatures may have developed under better-drained soil conditions. Such divergent soil conditions likely resulted from seasonal changes in hydrology as well large events such as storms that may have influenced the dispersion of organic matter.

Geochronology: The porcellanite bed with a zircon age of 254.73 ± 0.24 Ma at the 65 m stratigraphic level indicates that Blauwwater Farm 87 is a late Wuchiapingian locality. The Wuchiapingian spans the time between 259.8 ± 0.4 Ma and 254.14 ± 0.07 Ma (Fig. 9). This age contradicts a report by Ward et al. (2000) that indicates the section has the PTB, which is dated at 252.17 ± 0.06 Ma (Shen et al., 2011). They inferred the boundary based on a lithological transition from green to red siltstone, and the presence

SOME CONTEXT IN THE STRATIGRAPHY WOULD BE USEFUL FOR THE READER

IS THIS THE ONLY ENVIRONMENT IN WHICH THESE CAN FORM?

OUT OF LOGICAL SEQUENCES

of ^alamine interval. The discrepancy suggests that the lithological transition model used to trace the PTB across the central Karoo Basin is invalid.

Biostratigraphy: The zircon age also confirms that the *Dicynodon lacerticeps* skull in the section is latest Permian in age. The skull was collected at 81 m up section, which is 16 m above the zircon age of 254.73 ± 0.24 Ma. This zircon age falls within the *Dicynodon* AZ, which spans ~3 million years before the Permian-Triassic extinction (Rubidge et al., 2013, their Fig.2). The *Dicynodon* skull finding in accord with published vertebrate biostratigraphic models that used the *Dicynodon* Assemblage Fauna to define the latest Permian vertebrate biozone across the Karoo Basin (Smith, 1995; Ward & Smith, 2001; Rubidge et al., 2013).

VI. CONCLUSION

The majority of exposures at Blauwwater, Eastern Cape Province, South Africa occur as olive-gray or greenish-gray siltstone. The sedimentology is dominated by four main facies associations: (i) very fine-grained sandstone, (ii) sandy siltstone, (iii) lenticular siltstone, and (iv) homogenous siltstone. The very fine sandstone facies association is mainly attributed to channel deposits of likely high sinuosity fluvial systems (Smith, 1995; Ward et al., 1995). The sandy siltstone facies is interpreted as sandy channel fills, and represent low energy conditions and deposition from suspension ^{Load} during channel abandonment. The lenticular siltstone facies are floodplain overbank deposits. They are attributed to deposition from extensive overflow of fluvial systems during the Late Permian. The homogenous siltstone facies association is interpreted as paleosols ^{that include} gleysols and calcisols. Lithological indicators such as carbonate-cemented nodules, color mottling and soft sediment deformation structures

↘ AGAIN - SEE PREVIOUS COMMENTS

support the formation of homogenous siltstone facies under fluctuations from seasonal wet conditions to seasonally dry paleoclimatic conditions.

A zircon age of 254.73 ± 0.24 Ma from a porcellanite bed at the 65 m stratigraphic level indicates that Blauuwater is a Wuchiapingian locality. It also indicates that a *Dicynodon lacerticeps* skull, collected at the 81 m stratigraphic level, is a late Permian vertebrate. This in turn confirms that the *Dicynodon* AZ can be used to define the latest Permian vertebrate biozone, as indicated by published vertebrate biostratigraphic models (Rubidge et al., 2013). Both the zircon age and *Dicynodon lacerticeps* skull indicate that the color transition to maroon siltstone at the 121 m stratigraphic level occurs within the *Dicynodon* AZ in the Wuchiapingian. This suggests that the lithological model used to mark the PTB at Blauuwater is questionable.

VII. ACKNOWLEDGEMENTS

National Science Foundation Grant EA 1123570, S.D. Bechtel, Jr. Foundation Summer Research Grant, Colby College Dean of Faculty office, and Colby College Department of Geology.

Thanks to Billy De Klerk, Albany Museum, Christian Kammerer, American Museum of Natural History, Tara Chizinski, Kody Spencer, Colby College, Valerie Nxumalo, Council for Geoscience.

VIII. CITED REFERENCES

- Benton, M.J., 1995, Diversification and Extinction in the History of Life: Science, v. 268, n. 5207, p. 52- 58.
- Berner, R.A., 2002, Examination of hypotheses for the Permo-Triassic boundary extinction by carbon cycle modeling: Proceedings of the National Academy of Sciences. USA, v. 99, p. 4172-77.
- Black, B.A., Elkins-Tanton, L.T., Rowe, M.C., Ukstins-Peate, I., 2012, Magnitude and consequences of volatile release from the Siberian Traps: Earth and Planetary Science Letters. v. 317, p. 363- 73.
- Brown, S.L., Hierman, P.R., Mehrrens, C.J., and Lini, A., 1998, Terrigenous layers in lake cores document fluctuations in New England's Holocene climate: GSA Abstracts with Programs, v. 81, p. 2523- 2524.
- Catuneanu, O., Wopfner, H., Eriksson, P.G., Cairncross, B., Rubidge, B.S., Smith, R.M.H., Hancox, P.J., 2005, The Karoo basins of south-central Africa: Journal of African Earth Sciences, v. 43, p 211- 253.
- Coney, L., Reimold, W. U., Hancox, P. J., Mader, D., Koeberl, C., McDonald, I., Vajda, V., and Kamo, S. L., 2007, Geochemical and mineralogical investigation of the Permian-Triassic boundary in the continental realm of the southern Karoo Basin, South Africa: Palaeoworld, v. 16(1), p 67- 104.
- De Kock, M.O., and Kirschvink, J.L., 2004, Paleomagnetic Constraints on the Permian-Triassic Boundary in Terrestrial Strata of the Karoo Supergroup, South Africa: Implications for Causes of the End-Permian Extinction Event: Gondwana Research, v. 7, p. 175- 183.
- Gastaldo, R.A., Neveling, J., Clark, C.K., and Newbury, S.S., 2009, The terrestrial Permian-Triassic boundary event bed is a non-event: Geology, v. 37, n. 3, p. 199- 202.
- Gerstenberger, H., and Haase, G., 1997, A highly effective emitter substance for mass

THESE ARE
OTHER PEER
REVIEWED PAPERS
that would have been cited

spectrometric Pb isotope ratio determinations: *Chemical Geology*, v. 136, p. 309- 312.

Jaffey, A.H., Flynn, K.F., Glendenin, L.E., Bentley, W.C., and Essling, A.M., 1971, Precision measurement of half-lives and specific activities of ^{235}U and ^{238}U : *Physical Review*, v. 4, p. 1889- 1906.

Johnson, M. R., Van Vuuren, C. J., Hegenberger, W. F., Key, R., & Show, U., 1996, Stratigraphy of the Karoo Supergroup in southern Africa: an overview: *Journal of African Earth Sciences*, v. 23(1), p. 3- 15.

Johnson, M.R., 1976, Stratigraphy and sedimentology of the Cape and Karoo Sequences in the Eastern Cape Province. PHD Thesis: Rhodes University, Grahamstown, p. 336

Johnson, M.R., van Vuuren, C.J., Visser, J.N.J., Cole, D.I., Wickens, H. de V., Christie, A.D.M., Roberts, D.L., and Brandl, G., 2006, Sedimentary rocks of the Karoo Supergroup: *Geological Society of South Africa*, p. 461–499.

Krogh, T.E., 1973, A low contamination method for hydrothermal decomposition of zircon and extraction of U and Pb for isotopic age determinations: *Geochimica et Cosmochimica Acta*, v. 37, p. 485- 494.

Lindeque, A., de Wit, M. J., Ryberg, T., Weber, M., & Chevallier, L., 2011, Deep crustal profile across the southern Karoo Basin and Beattie Magnetic Anomaly, South Africa: an integrated interpretation with tectonic implications: *South African Journal of Geology*, v. 114(3-4), p. 265- 292.

Ludwig, K.R., 2003, User's manual for Isoplot 3.00: A geochronological toolkit for Microsoft Excel: Berkeley Geochronology Center, Special Publication, n. 4, p. 71.

Mack, G. H., James, W. C., & Monger, H. C., 1993, Classification of paleosols: *Geological Society of America Bulletin*, v. 105(2), p. 129- 136.

Mattinson, J.M., 2005, Zircon U-Pb chemical abrasion ("CA-TIMS") method: combined annealing and multi-step partial dissolution analysis for improved precision and accuracy of zircon ages: *Chemical Geology*, v. 220, p. 47- 66.

Payne, J. L., and Clapham, M. E., 2012, End-Permian mass extinction in the oceans: An ancient analog for the twenty-first century?: *Annual Review of Earth and Planetary Sciences*, v. 40, p. 89- 111.

Retallack, G. J., Jahren, A. H., Sheldon, N. D., Chakrabarti, R., Metzger, C. A., and Smith, R. M. H., 2005, The Permian-Triassic boundary in Antarctica: *Antarctic Science-Institutional Subscription*, v. 17(2), p. 241- 258.

NOT PROPERLY
ORDERED

I'VE READ THE ORIGINAL - HAVE YOU?
IF NOT, THIS SHOULD NOT BE CITED.

OUT
of
ORDER

Retallack, G.J., Smith, R.M.H., and Ward, P.D., 2003, Vertebrate extinction across Permian-Triassic boundary in Karoo Basin, South Africa: Geological Society of America Bulletin, v. 115, p. 1133- 1152.

Rubidge, B. S., Erwin, D. H., Ramezani, J., Bowring, S. A., and de Klerk, W. J. 2013, High-precision temporal calibration of Late Permian vertebrate biostratigraphy: U-Pb zircon constraints from the Karoo Supergroup, South Africa: Geology, 41(3), p. 363- 366.

Rüst, B. R., and Nanson, G. C., 1989, Bedload transport of mud as pedogenic aggregates in modern and ancient rivers: Sedimentology, v. 36 (2), p. 291- 306.

Sanz, A., Garcia-Gonzalez, M. T., Vizcayno, C., and Rodriguez, R., 1996, Iron-manganese nodules in a semi-arid environment: Soil Research, v. 34(5), p. 623- 634.

Sheldon, N. D., and Tabor, N. J., 2009, Quantitative paleoenvironmental and paleoclimatic reconstruction using paleosols: Earth-Science Reviews, v. 95(1), p. 1- 52.

Shen, S.Z., Crowley, J.L., Wang, Y., Bowring, S.A., Erwin D.H., 2011, Calibrating the end-Permian mass extinction: Science, v. 334, p. 1367- 72.

Smith, R.H.M., 1990, Alluvial Paleosols and Pedofacies Sequences in the Permian Lower Beaufort of the Southwestern Karoo Basin, South Africa: Journal of Sedimentary Research, v. 60, p. 258- 276.

Smith, R.M.H., 1995, Changing fluvial environments across the Permian-Triassic boundary in the Karoo basin, S. Africa and possible causes of tetrapod extinctions: Paleogeography, Paleoclimatology, Paleoecology, v. 117, p. 81- 104.

Smith, R.M.H., and Ward, P.D., 2001, Pattern of vertebrate extinctions across an event bed at the Permian-Triassic boundary in the Karoo Basin of South Africa: Geology, v. 28, p. 227- 230.

Smith, R.H.M., 1993, Sedimentology and Ichnology of paleosurfaces in the Beaufort Group (Late Permian), Karoo Basin, South Africa: PALAIOS, v. 8, p. 339- 357.

Spencer, K., Gastaldo, A., Neveling, J., Geissman, J., Prevec, R., Kamo, S., 2013, The late Permian stratigraphy of the Basal Tweefontein section, Eastern Cape Province, South Africa: Geological Society of America Abstracts with Programs, v. 45, n. 7, p. 127.

Tabor, N.J., Montanez, I.P., Steiner, M.B., Schwindt, D., 2007, $\delta^{13}\text{C}$ values of carbonate nodules across the Permian-Triassic boundary in the Karoo Supergroup (South Africa) reflect a stinking sulfurous swamp, not atmospheric CO_2 : Paleogeography, Paleoclimatology, Paleoecology, v. 252(1), p. 370- 381.

✓ Twitchett, R.J., Looy, C.V., Morante, R., Visscher, H., Wignall, P.B., 2001, Rapid and synchronous collapse of marine and terrestrial ecosystems during the end-Permian biotic crisis: *Geology*, v. 29, p. 351– 54

Ward, P.D., Botha, J., Buick, R., Dekock, M.O., Erwin, D.H., Garrison, G., Kirschvink, J., and Smith, R.H.M., 2005, Abrupt and gradual extinction among Late Permian Land Vertebrates in the Karoo Basin, South Africa: *Science*, v. 307, p. 709- 714.

Ward, P.D., Montgomery, D.R., and Smith, R.M.H., 2000, Altered river morphology in South Africa related to the Permian-Triassic extinction: *Science*, v. 289, p. 1740- 1743.

✓ Wright, V. P., 1992, Paleosol recognition: a guide to early diagenesis in terrestrial settings: *Developments in Sedimentology*, v. 47, p. 591- 619.

✓ Wright, V. P., and Marriott, S. B., 1996, A quantitative approach to soil occurrence in alluvial deposits and its application to the Old Red Sandstone of Britain: *Journal of the Geological Society*, v. 153, p. 1- 7.

Siltstone		
Lithology #	Grain Size	Color
1	Fine & Coarse	Olive-gray (5Y 4/1), Brownish-gray (5YR 4/1), Greenish-gray (5GY 6/1)
2	Sandy Coarse	Shades of Olive-gray (5Y 4/1) or Greenish-gray (5GY 6/1)
Sandstone		
3	Very Fine Sandstone	Greenish-gray (5GY 6/1), Light olive gray (5Y 5/2), Vey Pale Brown (10YR 8/3)

TABLE 1. Lithologies identified based on field and laboratory grain size and color descriptions.

Samp le #	Strat. Level (m)	Lithol ogy	Sand: Silt	Q %	F %	L %	Avg. Φ Size	Sorting σ	Kurto sis
19.01.5	56	VFSS	84:16	59	11	31	3.35	0.37	0.89
16.01.1	68	VFSS	77:23	39	17	45	3.01	0.53	0.13
16.01.2	108	VFSS	74:26	61	12	27	3.08	0.5	-0.54
19.01.7	116.5	VFSS	80:20	57	11	32	3.5	0.31	-0.52

TABLE 2. Thin section data showing sandstone sample sand to silt ratios, QFL proportions, Average Phi grain sizes, sorting standard deviation, and kurtosis. All data were collected from 300-grain counts per slide in transects.

LITHOFACIE SFACIES	GRAIN SIZE	COLOR	FEATURES
Very fine-grained Sandstone	Very fine Sand	Greenish-gray (5GY 6/1), Light olive gray (5Y 5/2), Very Pale Brown (10YR 8/3)	Laminae, mm-scale cross-beds, asymmetrical ripples, and soft deformations, abundant organics, moderate to well sorting, and higher quartz component
Sandy Siltstone	Sandy Coarse Silt	Olive-gray (5Y 4/1) or Greenish-gray (5GY 6/1)	Bands of sand and silt, sandstone lenses and siltstone lamina, isolated climbing dune, angular mud pebbles, erosional bases and sharp tops
Lenticular Siltstone	Fine & Coarse Silt	Olive-gray (5Y 4/1), Brownish-gray (5YR 4/1), Greenish-gray (5GY 6/1)	Lenticular beds, mm-scale parallel laminations, planar cross-beds, ripples, absence of nodules and color mottling
Homogenous Siltstone	Fine & Coarse Silt	Olive-gray (5Y 4/1), Brownish-gray (5YR 4/1), Greenish-gray (5GY 6/1)	Massive, homogenous bedforms, extensive bioturbation, mud-draped bedding, organic matter, carbonate cemented nodules, color mottling, rare cross-laminated lenses

TABLE 3. Lithofacies based on a compilation of field and laboratory descriptions of grain sizes, geometries, and sedimentary and biogenic structures.

Strat Level (m)	Sample ID	Carbon	Nitrogen	TOC:TON	Strat Level (m)	Sample ID	Carbon	Nitrogen	TOC:TON
127.7	50	0.26	0.087	3	123.2	20	0.19	0.063	3.05
127.55	49	0.14	0.053	2.56	123.05	19	0.21	0.033	6.2
127.4	48	0.26	0.073	3.59	122.9	18	0.24	0.047	5.21
127.25	47	0.16	0.047	3.5	122.75	17	0.15	0.05	3
127.1	46	0.16	0.076	2.11	122.6	16	0.16	0.053	2.94
126.95	45	0.12	0.037	3.27	122.45	15	0.21	0.056	3.76
126.8	43	0.93	0.053	17.5	122.3	14	0.17	0.06	2.89
126.65	44	0.24	0.043	5.46	122.15	13	0.16	0.053	3.06
126.5	42	0.19	0.053	3.56	122	12	0.19	0.063	3.05
126.35	41	0.19	0.04	4.75	121.85	11	0.14	0.043	3.31
126.2	40	0.43	0.096	4.48	121.7	10	0.16	0.053	2.94
126.05	39	0.15	0.047	3.29	121.55	9	0.22	0.057	3.94
125.9	38	0.25	0.06	4.22	121.4	8	0.18	0.076	2.35
125.75	37	0.183	0.076	2.39	121.25	7	0.27	0.083	3.59
125.6	36	0.15	0.07	2.07	121.1	6	0.11	0.34	0.33
125.45	35	0.21	0.063	3.37	120.95	5	0.32	0.09	3.59
125.3	34	0.18	0.06	3.06	120.8	4	0.15	0.045	3.3
125.15	33	0.18	0.07	2.57	120.65	3	0.13	0.045	2.89
125	32	0.13	0.073	1.77	120.5	2	0.23	0.04	5.87
124.85	31	0.27	0.063	4.26	120.35	1	0.16	0.065	2.46
124.7	30	0.17	0.047	3.71	115.5	19.01.8	0.29	0.073	4
124.55	29	0.17	0.043	3.85	114	19.01.9	0.37	0.092	4.11
124.4	28	0.22	0.05	4.4	68	19.01.6	0.75	0.017	45.1
124.25	27	0.17	0.04	4.33	47	19.01.4	0.35	0.02	17.33
124.1	26	0.14	0.037	3.91	42	19.01.3	0.32	0.045	7.11
123.95	25	0.18	0.083	2.16	38	19.01.2	0.62	0.068	9.2
123.8	24	0.22	0.057	3.88					
123.5	22	0.13	0.023	5.43					
123.35	21	0.17	0.057	3.85					

TABLE CAPTION?
NEXT PAGE

TABLE 4. TOC, TON values are shown with their corresponding stratigraphic positions. Values <10 indicate algal organic matter signatures, whereas values >20 indicate strongly terrestrial plant organic matter signatures. Most values are <10, with the exception of highlighted values, indicating the presence of terrestrial plant organic matter signatures.

INSERT
HARD PAGE BREAK
NOT adding lines!!

FOR 11 FIGURES?
163MB!! FOR THE
FIGURES ?? THESE
SHOULD HAVE BEEN
REMOVED USING PHOTOSHOP

(A)
WHITE
CIRCLE /
BLACK
LETTERS

(B)

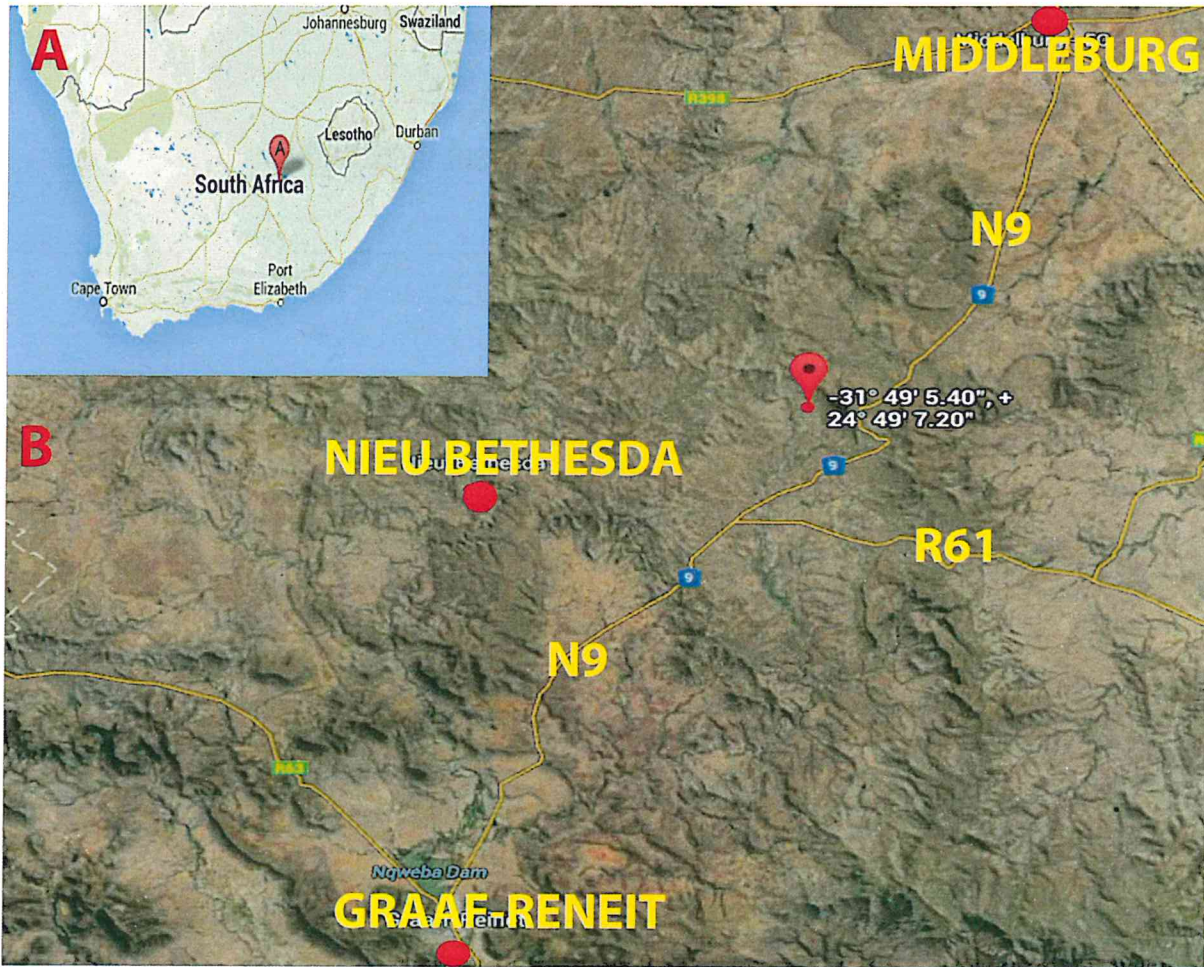


FIG 1. – Locality map for Blauwwater Farm 87, Eastern Cape Province, South Africa. **A:** An overview map of South Africa, showing the location of Blauwwater Farm 87 (Red drop pin). **B:** GPS Coordinates ($S31^{\circ} 49.090$, $E24^{\circ} 49.120$ – marked by red drop pin) of Blauwwater Farm 87. The locality is located in between three towns (marked by red dots): Graaf-Reinet, Middleburg, and Nieu Bethesda, and west of the N9 and R61 highways.

INSERT: HARD PAGE BREAK

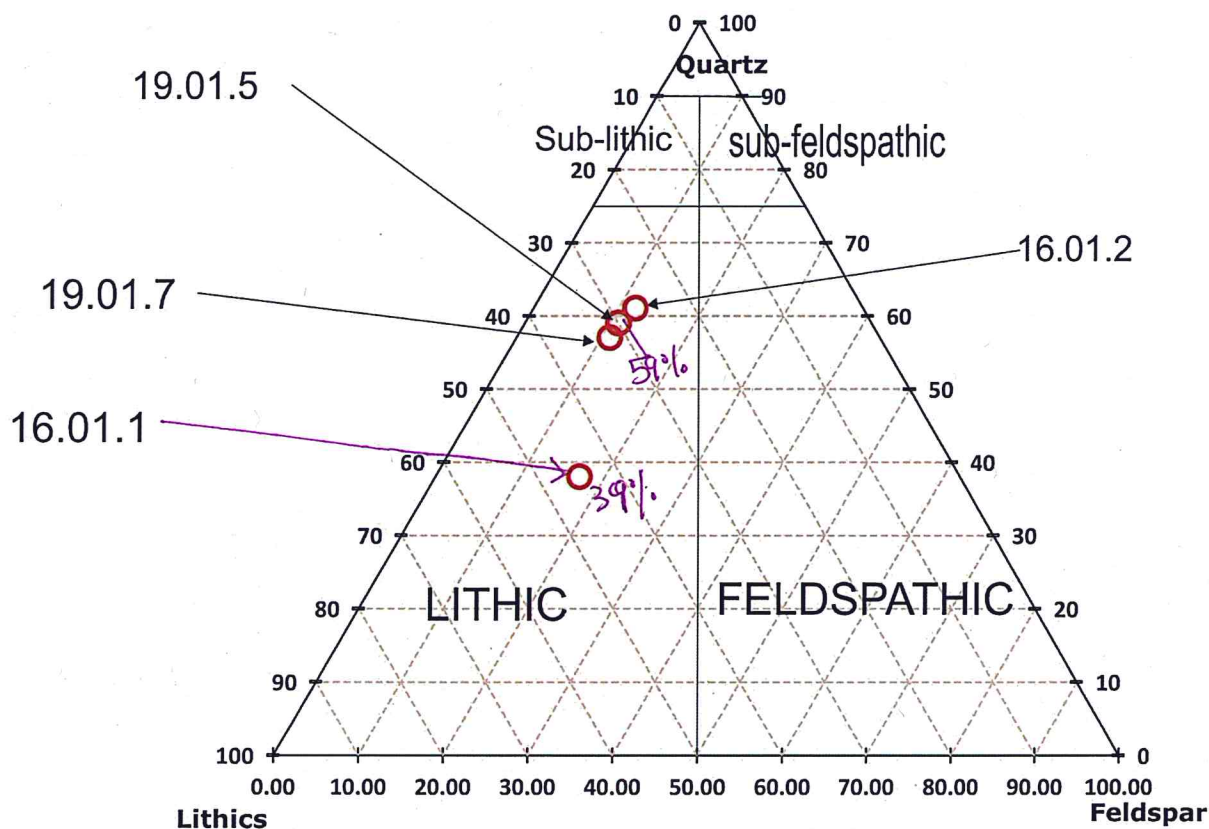
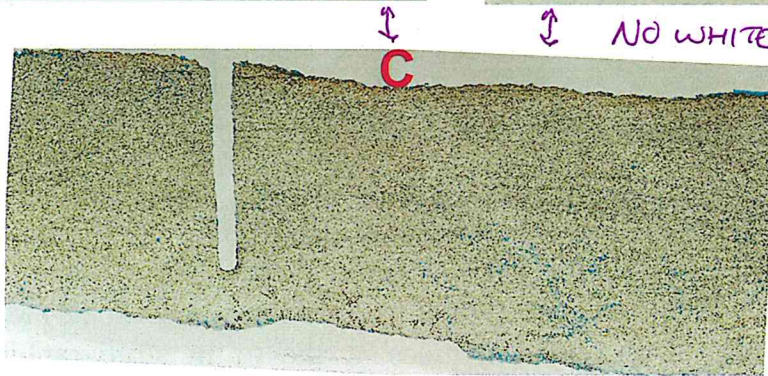
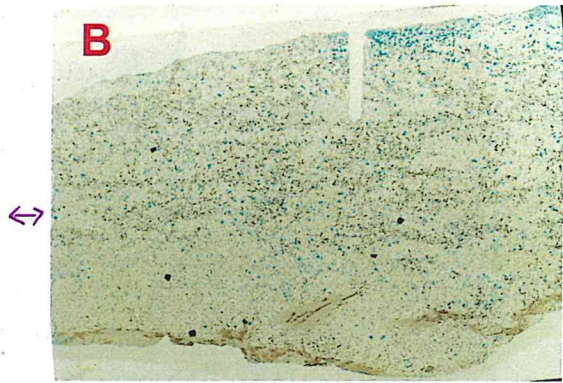
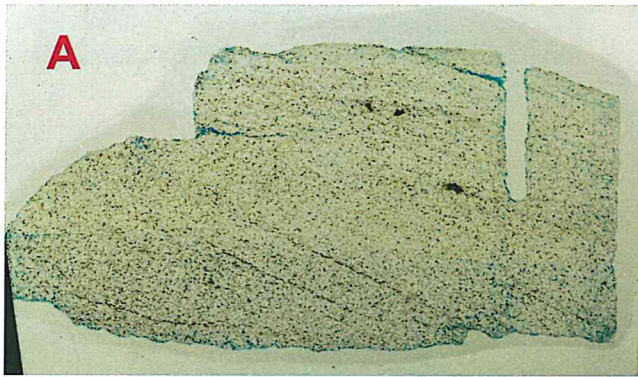


FIG 2. A ternary diagram constructed from 300 point-count analyses for sandstone samples (TABLE 2). All sandstones fall in the lithic field.



↔

↕

↕

NO WHITE SPACES IN A
A PROFESSIONAL
FIGURE

Figure 3

FIG3. Photographs of thin sections from the upper interval at Blauwwater Farm 87. **(A)** Cross-beds in a very fine sandstone at the 56 m stratigraphic level. **(B)** A bioturbated coarse siltstone from a stratigraphic height of 117 m. **(C)** Ripples in sandy coarse siltstone at the 68 m stratigraphic height.

Homogenous? (p.17)

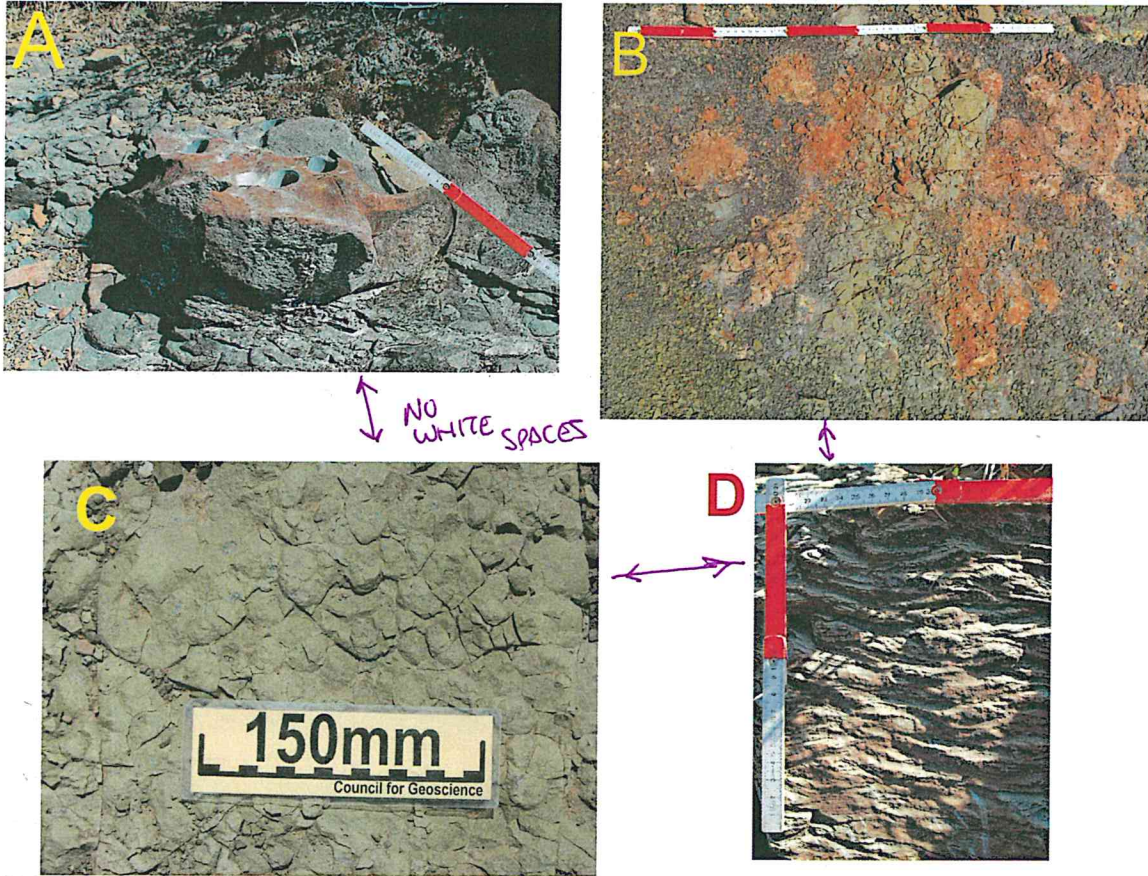
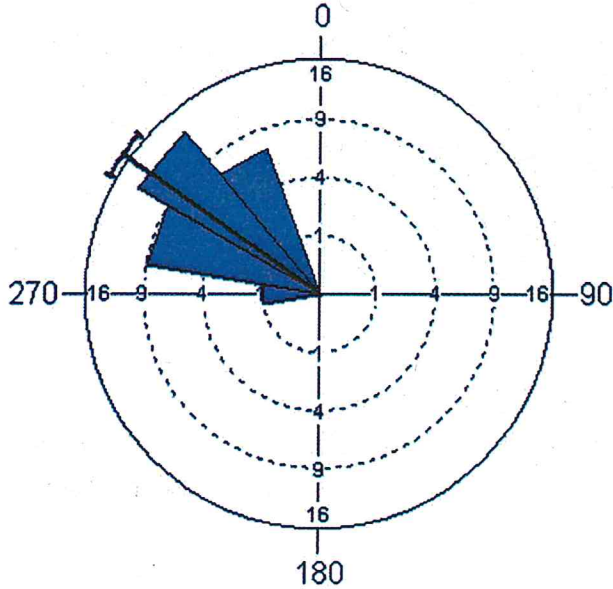


Figure 4. Photographs of pedogenic features and primary structures commonly found within the upper interval at Blauwwater Farm 87. (A) A smooth-topped, brown carbonate-cemented nodule found at the 52 m stratigraphic level. (B) Mottled siltstones surrounding carbonate-cemented nodules at the 91 m stratigraphic position. (C) Millimeter-scale mud clasts found in a sandy coarse siltstone at a stratigraphic height of 34 m. (D) Trough cross-beds at the 55 m level. *Scale??*

THIS IS A DATA TABLE AND NOT A FIGURE -

Paleocurrent Direction



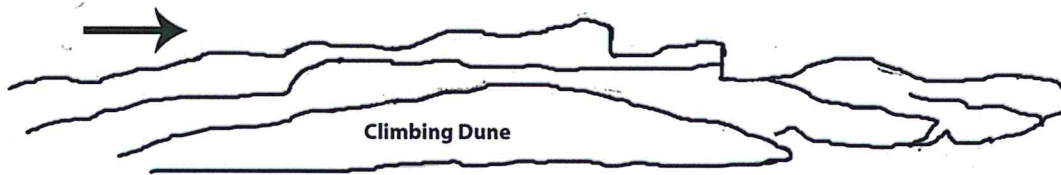
BASIC STATISTICS	
Upper tweefontein paleocurrent	
Analysis begun: Monday, July 09, 2012 8:59:23 AM	
Variable	Angles
Data Type	Angles
Number of Observations	30
Mean Vector (μ)	307
Length of Mean Vector (r)	0.96
Median	305
Concentration	14
Circular Variance	0.04
Circular Standard Deviation	16
Standard Error of Mean	3.4
95% Confidence Interval (-/+ for μ)	300.42
	314
99% Confidence Interval (-/+ for μ)	298
	316
Rayleigh Test (Z)	19
Rayleigh Test (p)	1E-08
Rao's Spacing Test (U)	282
Rao's Spacing Test (p)	< 0.01

WHAT DO THESE MEAN? YOU HAVE NOT USED THEM IN THE PAPER YET PRESENT THEM WITHOUT EXPLANATIONS

BELONGS AS A TABLE WITH SEPARATE CAPTION

Figure 5. A rose diagram and table based on 30 measurements of trough cross-bed axes at the 57m stratigraphic level. The mean vector direction is 307° with a standard error of 3.4 degrees.

DEVIATION? of 16°



THIS IS
A
POOR
PHOTOMOSAIC

Figure 6. Photograph and tracing of an isolated climbing dune structure at a stratigraphic height 33 m. The red and black arrows show the paleocurrent direction

based
ON WHAT FEATURE?

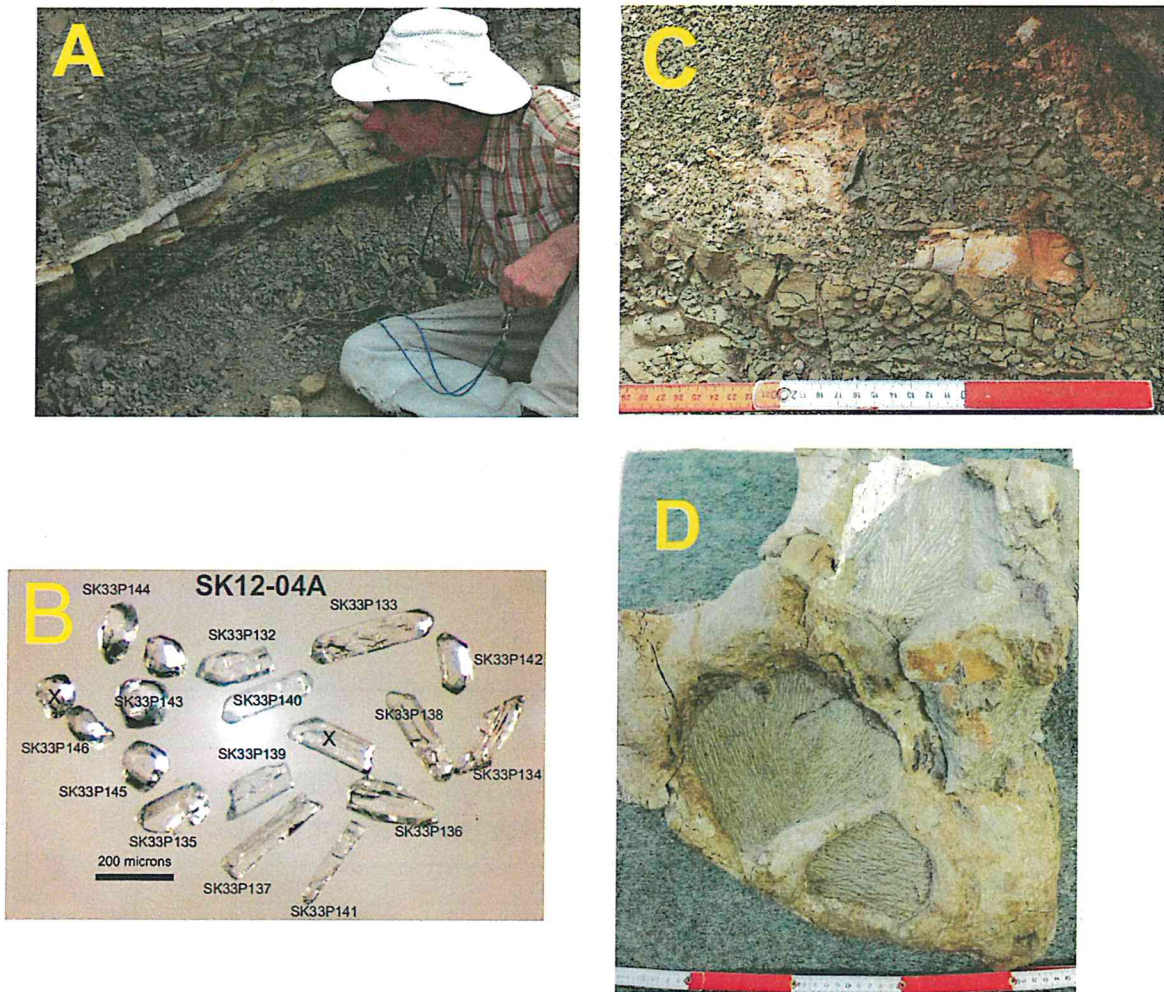


Figure 7. Photographs of a zircon bearing porcellanite and a *Dicynodon lacerticeps* skull before and after laboratory preparation. **(A)** John Geissman examining a zircon bearing porcellanite bed, which is located ~500 m west of the upper Blauwwater interval and correlative at a stratigraphic height of ~ 65 m. The GPS location of the skull is S31° 49.090 E24° 49.116 **(B)** Zircon crystals extracted from porcellanite bed for U-Pb isotopic analysis. The crystals are shown at a scale of 200 microns. **(C)** A *Dicynodon lacerticeps* skull before collection from a donga ~300 m west of the section and is correlative at stratigraphic height of 81 m. The GPS location of the skull is S31° 49.055 E24° 49.528. **(D)** *Dicynodon lacerticeps* skull after preparation by Billy De Klerk at the Albany Museum, and Christian Kammerer at the American Museum of Natural History.

identification by

SERIOUSLY?

HUH? I thought this was ABOUT THE PORCELLANITE

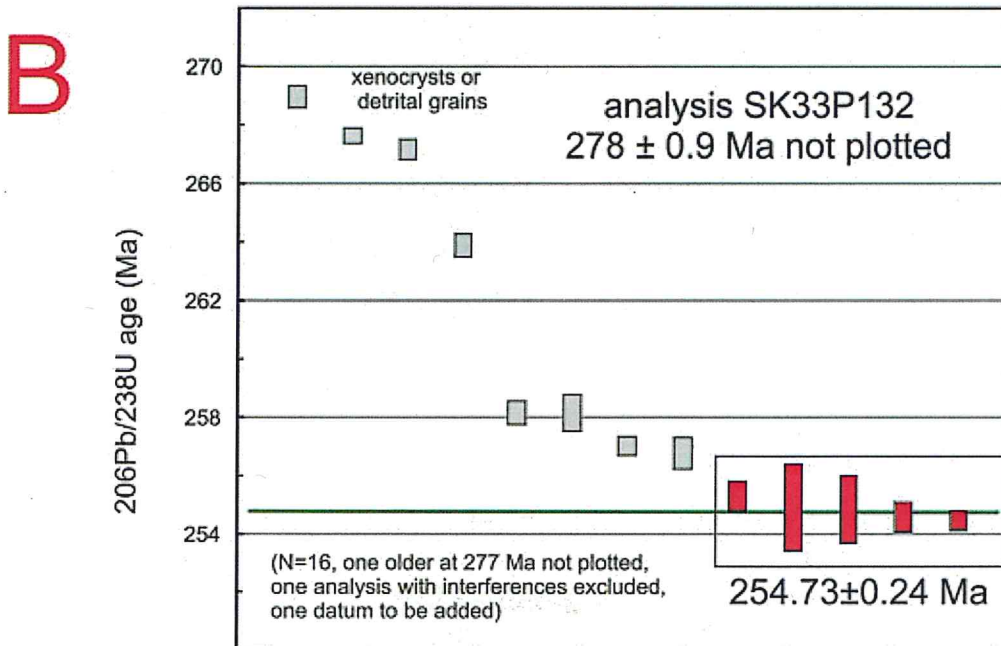
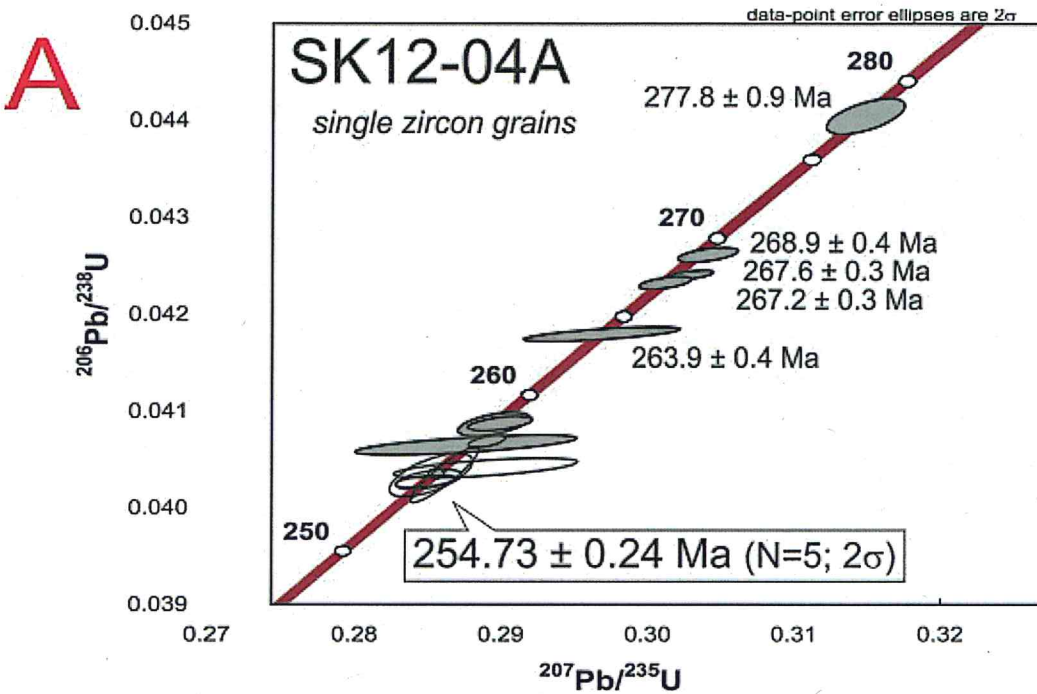
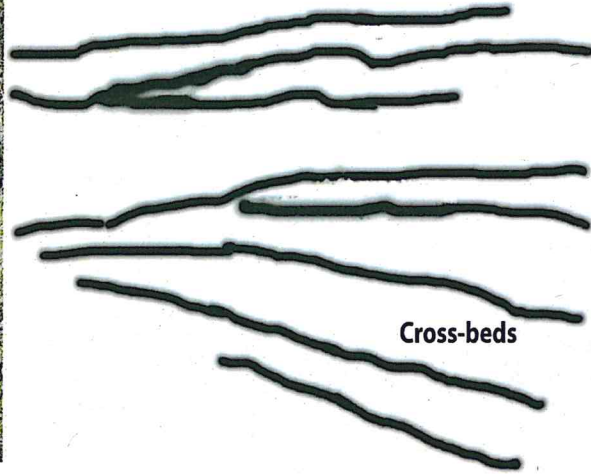


Figure 8. Concordia diagram and plots of $^{206}\text{Pb}/^{238}\text{U}$ zircon single grain ages from porcellanite bed (fig.7a, 7b). (A) Concordia diagram showing concordant single grain data. (B) Plots of $^{206}\text{Pb}/^{238}\text{U}$ single grain age. The youngest five data have a weighted mean age of $254.73 \pm 0.24 \text{ Ma}$ (2σ) and is interpreted as a maximum for the time of deposition of the unit.

Triassic	Upper	Rhaetian	201.3 ± 0.2	
		Norian	~ 208.5	
		Carnian	~ 227	
	Middle	Ladinian	~ 237	
		Anisian	~ 242	
	Lower	Olenekian	247.2	
		Induan	251.2	
		Changhsingian	252.17 ± 0.06	
	Permian	Lopingian	Wuchiapingian	254.14 ± 0.07
			Capitanian	259.8 ± 0.4
Guadalupian		Wordian	265.1 ± 0.4	
		Roadian	268.8 ± 0.5	
		Kungurian	272.3 ± 0.5	
Cisuralian		Artinskian	283.5 ± 0.6	
		Sakmarian	290.1 ± 0.26	
		Asselian	295.0 ± 0.18	
			298.9 ± 0.15	

Figure 9. Permian-Triassic subdivisions according to the International Commission on Stratigraphy (ICS, 2013). The Wuchiapingian spans the time between 259.8 ± 0.4 and 254.14 ± 0.07 Ma.

MISSING
CITATION
IN
REFERENCES



THIS IS
VERY
COARSE
WITHOUT A
SCALE
to
compare
with the
IMAGE

Figure 10. Photograph and tracing of cm-scale cross beds in a very fine sandstone at the 56 m stratigraphic level.

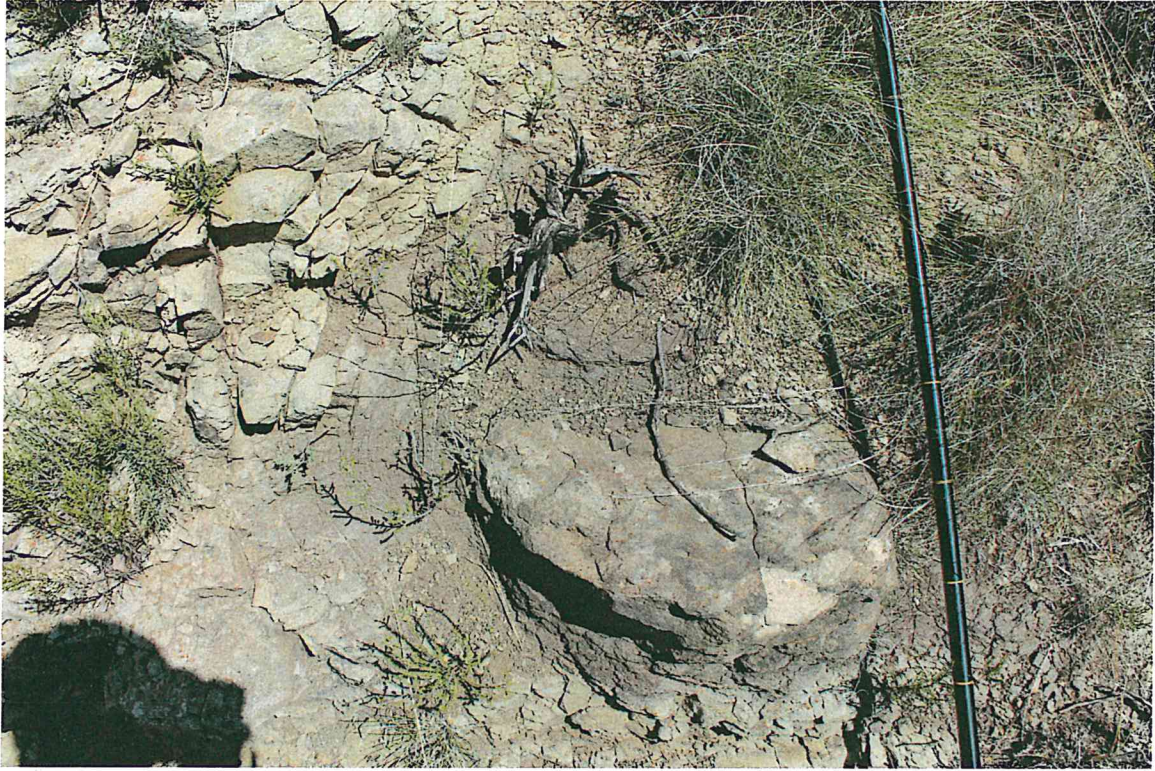


Figure 11. Photograph of soft sediment deformation structure in a very fine sandstone interval at the 84 m stratigraphic height.

How ABOUT AN ARROW TO DIRECT
THE READER'S ATTENTION?
How ABOUT A SCALE?

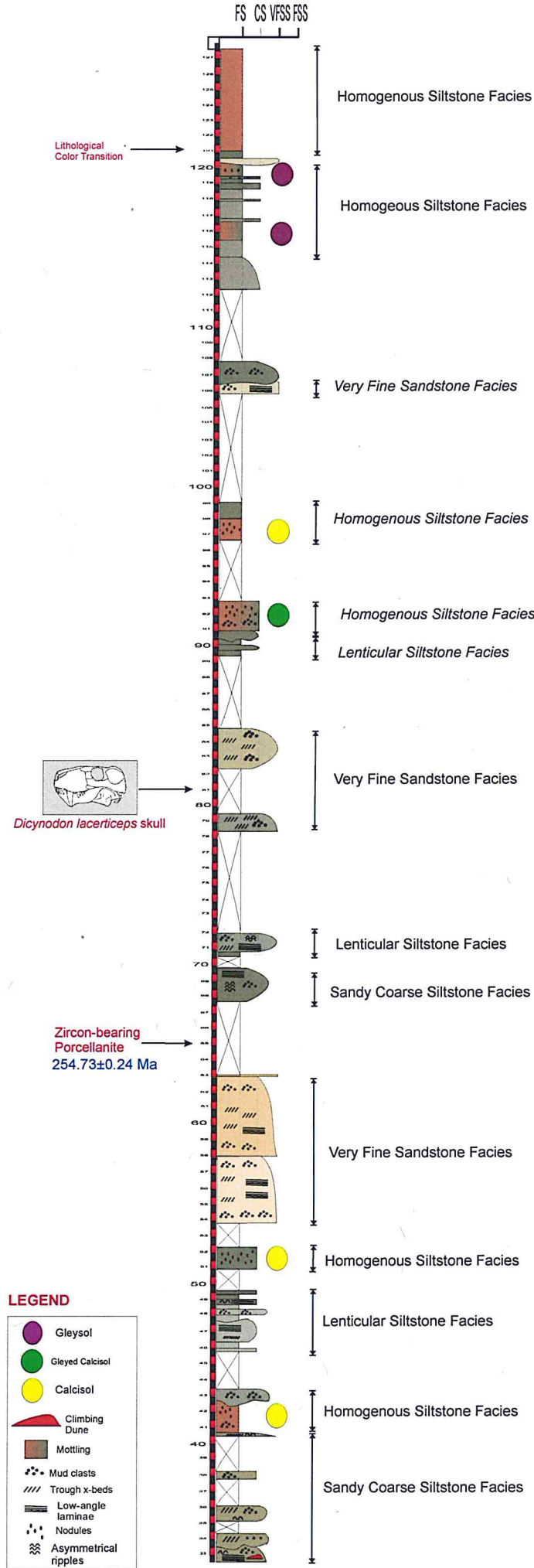
Figure 12: See attached stratigraphic column.

WHY IS THE FILE SO LARGE?



STRATIGRAPHIC
SECTION

THIS COULD HAVE BEEN
SEALED APPROPRIATELY
TO 14" x 40" PAPER SIZE
AND THEN PRINTED ONTO
AN 8 1/2" x 11 SHEET AS
ATTACHED FOR REVIEW



WHAT ARE THE INTERPRETED DEPOSITIONAL ENVIRONMENTS FOR THE LITHOFACIES THAT ARE NOT PEDOGENICALLY ALTERED?

HOW THICK ARE THE CHANNEL BEDDING AND CHANNEL FILL INTERVALS?